Draft version May 11, 2017

IMPLICATIONS FOR THE ORIGIN OF DWARF EARLY-TYPE GALAXIES: A DETAILED LOOK AT THE ISOLATED ROTATING DWARF EARLY-TYPE GALAXY LEDA 2108986 (CG 611), RAMIFICATIONS FOR THE FUNDAMENTAL PLANE'S S^2_K KINEMATIC SCALING AND THE SPIN–ELLIPTICITY DIAGRAM

Alister W. Graham, Joachim Janz
Centre for Astrophysics and Supercomputing, Swinburne University of Technology, Victoria 3122, Australia.

Samantha J. Penny
Institute of Cosmology and Gravitation, University of Portsmouth, Dennis Sciama Building, Burnaby Road, Portsmouth PO1 3FX, UK.

Igor V. Chilingarian
Smithsonian Astrophysical Observatory, 60 Garden Street MS09, Cambridge, MA 02138, USA.; Sternberg Astronomical Institute, Moscow State University, 13 Universitetsky prospect, Moscow 119992, Russia.

Bogdan C. Ciambur, Duncan A. Forbes
Centre for Astrophysics and Supercomputing, Swinburne University of Technology, Victoria 3122, Australia.

Roger L. Davies
Sub-department of Astrophysics, Department of Physics, University of Oxford, Denys Wilkinson Building, Keble Road, Oxford OX1 3RH, UK.

Draft version May 11, 2017

Abstract

Selected from a sample of nine, isolated, dwarf early-type galaxies (ETGs) with the same range of kinematic properties as dwarf ETGs in clusters, we use LEDA 2108986 (CG 611) to address the Nature versus Nurture debate regarding the formation of dwarf ETGs. The presence of faint disk structures and rotation within some cluster dwarf ETGs has often been heralded as evidence that they were once late-type spiral or dwarf irregular galaxies prior to experiencing a cluster-induced transformation into an ETG. However, CG 611 also contains significant stellar rotation ($\approx$20 km s^{-1}) over its inner half-light radius ($R_{\rm e,maj}$ = 0.71 kpc), and its stellar structure and kinematics resemble those of cluster ETGs. In addition to hosting a faint young nuclear spiral within a possible intermediate-scale stellar disk, CG 611 has accreted an intermediate-scale, counter-rotating gas disk. It is therefore apparent that dwarf ETGs can be built by accretion events, as opposed to disk-stripping scenarios. We go on to discuss how both dwarf and ordinary ETGs with intermediate-scale disks, whether under (de)construction or not, are not fully represented by the kinematic scaling $S_{0.5} = \sqrt{0.5\,V^2_{\rm rot} + \sigma^2}$, and we also introduce a modified spin–ellipticity diagram $\lambda(R)$–$\epsilon(R)$ with the potential to track galaxies with such disks.

Keywords: galaxies: dwarf — galaxies: individual (CG 611) — galaxies: structure — galaxies: kinematics and dynamics — galaxies: formation — galaxies: evolution

1. INTRODUCTION

Dwarf early-type[1] galaxies (ETGs) — encompassing dwarf elliptical (dE), dwarf ellicular[2] (dES), and dwarf lenticular (dS0) galaxies — are commonly found in clusters of galaxies but are relatively scarce in the field. Building on van den Bergh (1976) and Butcher & Oemler (1978), it has been theorized that these low-mass galaxies were originally late-type spiral galaxies or irregular disk galaxies that were stripped of their gas (Gunn & Gott 1972; Larson et al. 1980) and then "harassed" and reshaped into ETGs by either a cluster environment (Moore et al. 1996, 1998; Mastropietro et al. 2005) or through "tidal stirring" by a massive neighbor (Mayer et al. 2001a, 2001b). While there is abundant observational evidence of gas-stripping (e.g. Gavazzi et al. 2001; Michielsen et al. 2008; Yagi et al. 2010; Owers et al. 2012; Merluzzi et al. 2013, 2016; Ebeling et al. 2014; Boselli et al. 2016), here we investigate the case for morphological transformation, specifically, whether rotation and (weak) disk structures in dwarf ETGs are actually proof of late-type galaxies transformed into dwarf ETGs — as is commonly advocated in the literature (e.g. Boselli et al. 2008; De Rijcke et al. 2010; Kormendy & Bender 2012; Penny et al. 2014; Benson et al. 2015; Ryś et al. 2015; Toloba et al. 2015; Janz et al. 2016).

Dwarf ETGs have typically been distinguished by low luminosities ($M_B > -18$ mag; $M_r \gtrsim -19.3$ mag) and

AGraham@astro.swin.edu.au

[1] Throughout this paper, the terms "early-type" and "late-type" are used in reference to a galaxy's stellar morphology, rather than its stellar population.

[2] The term "ellicular" was introduced in Graham et al. (2016) to describe the "ES" galaxy class (intermediate between E and S0) that was introduced by Liller (1966).

low stellar masses ($M_* < 5 \times 10^9\ M_\odot$), and the absence of wide-spread star formation. Furthermore, their lack of a large-scale spiral pattern voids their membership of the spiral, i.e. the late-type, galaxy class. A key reasoning in support of the galactic metamorphosis of ETGs from late-type galaxies has been the presence of a significant rotational component (e.g. Pedraz et al. 2002; Simien & Prugniel 2002; Geha et al. 2003; de Rijcke et al. 2005; Chilingarian et al. 2009; Geha et al. 2010; Toloba et al. 2015; Penny et al. 2016) which has typically been interpreted as a remnant of the initial disk from which these galaxies were supposedly transformed. However, most ordinary, i.e. non-dwarf, ETGs are also now known to contain a substantial rotating disk[3]. That is, they are not the purely pressure supported systems held up by random stellar motions that they were once considered to be. Measuring the major-axis kinematics of the brightest ETGs in the Fornax cluster, Graham et al. (1998) reported that "the true number of *dynamically hot* stellar systems is much lower than previously thought," a result also seen using 2D kinematic maps of Fornax ETGs (Scott et al. 2014) and confirmed in notably larger samples of ETGs beyond the Fornax cluster (Emsellem et al. 2011; Oh et al. 2016). However, many of these galaxies are too massive for "harassment" (of what was originally a spiral galaxy) to have been effective, and many are not even located in a cluster environment where "harassment" could have played its (harsh) nurturing hand.

If the rotating disks in ordinary ETGs have been built by accretion events, from either an initial primordial collapse and/or around a pre-existing spheroidal component (Graham et al. 2015, 2016; de la Rosa et al. 2016), then it somewhat undermines the above argument for a transformation scenario for the dwarf ETGs. Moreover, the kinematic properties of dwarf and ordinary ETGs display no sign of a divide at $M_B = -18$ mag (e.g. Norris et al. 2014; Penny et al. 2016) — which is the magnitude commonly used for the dwarf/ordinary naming convention but is also alleged to mark a separation about which distinct physical processes operate (Kormendy & Bender 2012, and references therein). Rather than a dichotomy of merger-built ordinary ETGs versus "harassed" late-type galaxies that have been transformed into dwarf ETGs, there is a continuity at $M_B = -18$ mag of physical properties such as the presence of disks, the occurrence of kinematic substructure, metallicity, metallicity gradients, globular cluster systems, mass-to-light ratios, etc. (e.g. Forbes et al. 1996, 2008; Graham & Guzmán 2003; Gavazzi et al. 2004; de Rijcke et al. 2005; Ferrarese et al. 2006; Côté et al. 2007, 2008; Janz & Lisker 2008, 2009; den Brok et al. 2011; Koleva et al. 2011; Weinmann et al. 2011; Ferrarese 2016). The luminosity-velocity dispersion relation is also continuous at $M_B = -18$ mag, with a logarithmic slope of 2 (e.g. Davies et al. 1983; Held et al. 1992; de Rijcke et al. 2005; Matković & Guzmán 2005; see also the historical review in section 3.3.3 of Graham 2013).

Continuing from Bender et al. (1992), Kormendy & Bender (2012) have claimed that the formation physics must be very different for dwarf ETGs fainter than $M_B = -18$ mag and ordinary ETGs brighter than $M_B = -18$ mag (see also Wirth & Gallagher 1984). To support this claim, they remark how these galaxies appear to follow different relations in diagrams involving effective half-light radii and/or effective surface brightnesses. However, as explained in Graham & Guzmán (2003, 2004) and Graham (2005), this is because of the use of these particular parameters produces a continuous but *curved* relation. The bend at around $M_B = -18$ mag, and the different slopes seen at the low- and high-luminosity ends, have little to do with the formation physics but are instead a consequence of "structural non-homology". That is, the bend is due to the continually changing radial concentration of light — which can be quantified through the use of the Sérsic (1963) index — as one moves along the ETG sequence in luminosity and mass. See Graham (2013, 2016) for a historical review and detailed explanation.

Characterizing the structure and kinematics of isolated, dwarf ETGs in the low-z universe will enable us to better address the origin of dwarf galaxies. Due to their isolation, they cannot be harassed and morphologically transformed late-type galaxies. Therefore, the detection of a rotating disk in these galaxies would undermine the alleged Sp/dIrr origin of dwarf ETGs in clusters. To reiterate that point, if field ETGs have acquired their rotation from their original growth into an early-type galaxy, i.e. Nature, then it removes the need for the transformation of late-type disk galaxies by either the cluster environment or a neighboring massive galaxy, i.e. Nurture, as the (sole) formation path for dwarf ETGs. We have undertaken such an observing campaign, and the results are presented in Janz et al. (2017). Here we provide a more detailed presentation for one of these galaxies — specifically, for the galaxy CG 611 — than can be afforded, or is necessary, for all of the survey galaxies. While the existence of just one isolated, rotating, dwarf ETG is sufficient to question the popular formation mechanism for the rotating dwarf ETGs in clusters, larger samples enable one to explore the extent of the over-lapping range of physical properties of cluster and isolated dwarf ETGs. The process of disk growth, and disk removal, can leave galaxies with disks of varying, intermediate, sizes. In this paper, we present some of the hitherto overlooked implications of this, and offer ways forward.

In Section 2 we present the data on CG 611, including its location, isolation, distance, brightness, and effective half-light parameters (Section 2.1). In Section 2.2 we present a sub-arcsecond resolution image, a color map, and a bulge/disk/etc. decomposition of the galaxy light. In Section 2.3, we present new Keck/`ESI` spectra and an investigation of the kinematic behavior within the galaxy's half-light radius. A discussion of this collective data is presented in Section 3.1. We then identify similar galaxies located in clusters (Section 3.2) and present the revelations that this galaxy provides in regard to the formation of dwarf (and ordinary) ETGs (Section 3.3.1). Building on this, in Section 3.3.2, we stress the problematic nature of representing galaxies with intermediate-scale disks as single points in the popular spin–ellipticity diagram used to classify their kinematic state as either a 'fast rotator' or 'slow rotator' (e.g. (Emsellem et al. 2007; Cappellari et al. 2007). We suggest a way for-

[3] ETGs brighter than $M_B \approx -21.25$ mag, or with stellar masses greater than $\approx 10^{11}\ M_\odot$, tend not to have disks.

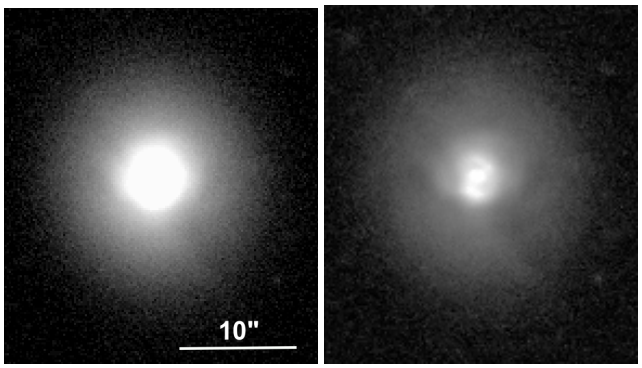

Figure 1. Left panel: *CFHT* r-band image of CG 611 ($R_{\rm e,gal} = 3''.2 = 0.71$ kpc). Right panel: manipulated unsharp-mask of the left panel to reveal the dust and inner structure. North is up and east is to the left in all images.

ward that accounts for both kinematic and ellipticity radial gradients where these galaxies transition from rotating fast where the disk dominates, to rotating slowly at larger radii. Finally, in Section 3.3.3, we discuss how studies are combining in quadrature the stellar rotation and the velocity dispersion from individual galaxies ($S_{0.5} = \sqrt{0.5\,V_{\rm rot}^2 + \sigma^2}$), but not yet using the sizes of the galaxy components (disk and spheroid) associated with these kinematic terms. We provide a brief summary in Section 4, which includes a list of future observations that could help to further this area of research.

2. DATA

Aside from being found in galaxy clusters, dwarf ETGs also exist in galaxy groups (e.g. NGC 205 in the Local Group: Monaco et al. 2009; Saviane et al. 2010) and in isolation. Although not commonplace, dozens of isolated dwarf ETGs are known (e.g. Karachentseva et al. 2010; Fuse et al. 2012). Building on the type of survey performed by Paudel et al. (2014), one of us (S.J.P.) has recently found 46 isolated dwarf ETGs with masses less than 5×10^9 $M_\odot$ and with redshifts $z < 0.02$. These have been tabulated in Janz et al. (2017). Rotation curves, obtained by one of us (J.J.), are presented there for nine of those galaxies with $M_B \lesssim -18$ mag. Here we report in some detail on one of those 46 dwarf ETGs: CG 611.

2.1. *Basic data*

LEDA 2108986 (R.A. = 15:03:15.57, decl. = +37:45:57.2, Paturel et al. 2003), previously cataloged by Sanduleak & Pesch (1987) as Case Galaxy[4] CG 611 and listed in the Reference Catalog of galaxy Spectral Energy Distributions (RCSED[5], Chilingarian et al. 2017) as object 588017627242758202, resides within the direction of the Bootes void.

Starting from the published *Sloan Digital Sky Survey* (SDSS) Data Release 3 (DR3: Abazajian et al. 2005) heliocentric radial velocity measurement for CG 611 of 2562±28 km s^{-1}, and adjusting for 'Virgo + Great-Attractor + Shapley' infall (Mould et al. 2000), we have an expansion velocity of 3140±37 km s^{-1} for CG 611. We assume a spatially flat universe (i.e. $\Omega_\Lambda + \Omega_m = 1$) with $\Omega_m = 0.308 \pm 0.012$ and a Hubble constant $H_0 = 67.8 \pm 0.9$ km s^{-1} Mpc^{-1} (Planck Collaboration et al. 2015). With this cosmology, the 'angular size distance' to CG 611 is 45.7 Mpc, which corresponds to a scale of 222 parsec per arcsecond (Wright 2006)[6]. The 'luminosity distance' is 46.7 Mpc, giving a (cosmological redshift corrected) distance modulus of 33.35 mag.

CG 611 has an SDSS Petrosian g'-band apparent magnitude of 15.44 mag (AB)[7]. After correcting for 0.052 mag of Galactic extinction in the g'-band toward CG 611 (from the Schlafly & Finkbeiner 2011 re-calibration of the Schlegel, Finkbeiner & Davis 1998 infrared-based dust map as reported by NED[8]), this corresponds to an absolute g'-band magnitude of −17.96 mag. The SDSS Petrosian r'-band apparent magnitude is 14.73 mag (AB), and the Galactic extinction corrected r'-band absolute magnitude is −18.66 mag (AB). The average $g' - r'$ galaxy color of 0.7 is typical of dwarf ETGs in the Virgo cluster (Janz & Lisker 2009).

From a single Sérsic fit, the published r'-band, major-axis, half-light radius $R_{\rm e,gal}$ is 3.2 arcsec, or 0.71 kpc (taken from the NASA Sloan Atlas[9], adopting the sky-subtraction method of Blanton et al. 2011), and the mean effective surface brightness is $\langle\mu\rangle_{\rm e,gal} = 19.22$ mag arcsec^{-2}. The published Sérsic index $n_{\rm gal} = 2.3$ is typical for a galaxy of this magnitude ($M_B \approx -18$ mag), placing it on the L–n diagram (see Figure 10 in Graham & Guzmán 2003).

Hernández-Toledo et al. (2010), Fuse et al. (2012) and Argudo-Fernández et al. (2015) have reported that CG 611 is an extremely isolated ETG. While Fuse et al. (2012) noted that there are no neighbors brighter than $M_V = -16.5$ mag within a projected co-moving distance of 2.5 Mpc and 350 km s^{-1} in redshift space, they did observe that there are two 'companion' galaxies fainter than $M_V = -16.5$ mag within the void that CG 611 resides. These galaxies have $M_{r'} = -15.7$ and −16.4 mag ($M_* \approx 0.5$–1.0×10^9 $M_\odot$) and are at projected distances of 2.5 and 2.8 Mpc, respectively, using our cosmological parameters given above.

From the NASA Sloan Atlas and the Two Micron All Sky Survey (2MASS) redshift survey (Huchra et al. 2012), we too have confirmed the isolation of CG 611. Within a projection of 1 Mpc, there are no known galaxies with a velocity difference of less than ±1000 km s^{-1} (using the environmental search tool in NED), and there is just one dwarf galaxy (with a heliocentric recessional velocity of 4037 km s^{-1}, and $M_{r'} = -17.5$ mag) within a projection of 2 Mpc. The closest 'neighbor' with a velocity difference of less than ±1000 km s^{-1} and which is brighter than $M_K = -23$ mag ($M_* \approx 10^{10}$ $M_\odot$) are the NGC 5899/NGC 5900 pair, at a projected distance of 3.9 Mpc away. The NGC 5929 Group is 5.6 degrees away on the sky, or 4.5 Mpc using a scale of 222 parsec per arcsecond.

2.2. *Imaging Data*

We have investigated archival *Canada France Hawaii Telescope* (*CFHT*)/MegaCam r-band images of the field containing CG 611 that were taken in mid-2011 by Cheng

[4] "Case" for Case Western Reserve University.
[5] http://rcsed.sai.msu.ru/catalog
[6] http://www.astro.ucla.edu/~wright/CosmoCalc.html
[7] In the g'-band, $M_{\odot,Vega} - M_{\odot,AB} = 0.1$.
[8] http://nedwww.ipac.caltech.edu
[9] http://www.nsatlas.org/

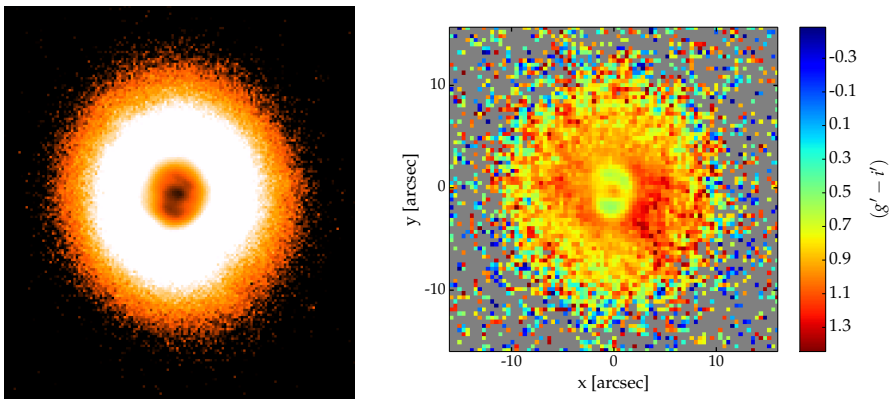

Figure 2. Left panel: false color *CFHT* r-band image to better reveal the inner bar and spiral. Right panel: SDSS $(g' - i')$-band color map of CG 611. Correcting for Galactic dust extinction makes the entire color map bluer by 0.025.

Li (Proposal Id 11BS09). The full width at half maximum (FWHM) for the point spread function (PSF) is $0.''8$ — measured from stars in the image. The galaxy is shown in the left panel of Figure 1, while the right panel shows a manipulated image to enhance the inner spiral and dust. If one was to strip out the dust (and gas), CG 611 would resemble other dwarf ETGs in clusters. A false color image is shown in Figure 2, providing our clearest view of the nuclear spiral pattern within the much larger elliptical stellar system.

While we do not rule out that the main body of this ETG may be a (thick) disk, as in S0 galaxies, it is easy to understand from the left panel of Figure 1 why this galaxy has been classified in the literature as an ETG. It is neither a dwarf irregular (dIrr) galaxy nor a late-type spiral galaxy in which the spiral arms extend to large radii. This may be a triaxial-shaped galaxy with an intermediate-scale disk that has grown a faint bar with spiral arms at the ends of it. Residing midway between E and S0 galaxies (with large-scale disk), such objects with intermediate-scale disks were designated as "ES" galaxies by Liller (1966). They have also been referred to as "disk ellipticals" (Nieto et al. 1988), "dEdi" galaxies if they are dwarfs (Lisker et al. 2006), and in Graham et al. (2016) the term "ellicular" was used to better capture the bridging nature between elliptical and lenticular galaxies.

2.2.1. *Color map*

Although we do not have sub-arcsecond imaging in two filters for CG 611, we have constructed a $(g' - i')$ color map using SDSS images (Figure 2). The color map reveals a number of things before becoming noisy at large radii.

The spiral arms have a blue SDSS $g' - i'$ color range of 0.5–0.6, commensurate with Sd–Sm type galaxies (Fukugita et al. 1995). The hot young stars that make the spiral arms shine blue likely account for the bulk of the ultraviolet radiation coming from this galaxy. The GALaxy Evolution eXplorer (*GALEX*) All-Sky Catalog based on *GALEX* General Release Six (Seibert et al. 2012)[10] reports an observed near-UV magnitude of 18.32 mag and a far-UV magnitude of 18.60 mag (AB) for CG 611.

In stark contrast to the arms, the surrounding spheroid is red and displays a gradient with less red colors at larger radii — a characteristic that is commonly observed in ETGs. Paudel et al. (2014) similarly report on a significant metallicity gradient — which is likely responsible for the color gradient — in another isolated compact ETG, which drops by 0.5–0.6 dex over the inner half-light radius (∼600 pc). We shall return to that galaxy in Section 3. For reference, large S0 and E galaxies have an average $g' - i'$ color of 1.0 and 1.2, respectively (Fukugita et al. 1995), while lower mass ETGs are somewhat bluer (e.g. Forbes et al. 2008, their Figure 1).

For completeness, we note that the 2MASS[11] (Jarrett et al. 2000) extended objects catalog reports a total K_s-band magnitude of 11.93 mag (Vega)[12] for CG 611. The galaxy was also observed by *WISE* (Wright et al. 2010) during the *WISE* full cryogenic mission. It has $m_{3.4} = 12.01$, $m_{4.6} = 12.02$, and $m_{12} = 8.42$ mag (Vega). Its red mid-infrared color $[4.6]-[12] = 3.6$ is consistent with dust heating, and places CG 611 on the region of the $[3.4]-[4.6]$ versus $[4.6]-[12]$ *WISE* color-color diagram occupied by spiral galaxies (e.g. Jarrett et al. 2011).

The innermost arcsecond is also red, suggesting the presence of a red bulge and/or bar having an older stellar age and/or higher stellar metallicity. This is not an artifact due to different seeing in either image because the better image (i'-band) was degraded (by convolution with a Gaussian) to match the seeing of the less-well-resolved image (g'-band). However, the presence of dust can act to redden the image.

In the color map, the dark red patch to the southwest of the spiral arms reaches a $g' - i'$ color of 1.3 to 1.4 and is likely due to dust. There is also evidence of a dark patch at this location in the r-band image, and the isophotes correspondingly pinch inward here. Two faint, parallel, dust lanes can also just be made out on the northeast quadrant. If not for the dust and the blue spiral arms, the $g' - i'$ color over the inner $\approx 2R_{\rm e,gal}$ is around 0.9, typical for an ETG of CG 611's brightness. This presence of the dust is interesting because it implies gas, and this is at a radius beyond the spiral arms; this is perhaps suggestive that the intermediate-scale disk and spiral may yet grow further. Obvious, but worth stating, is that if this disk grows sufficiently, it may transition to a large-scale disk and the galaxy might accordingly transition from an ES

[10] http://www.galex.caltech.edu/researcher/data.html

[11] http://www.ipac.caltech.edu/2mass

[12] 13.84 mag (AB).

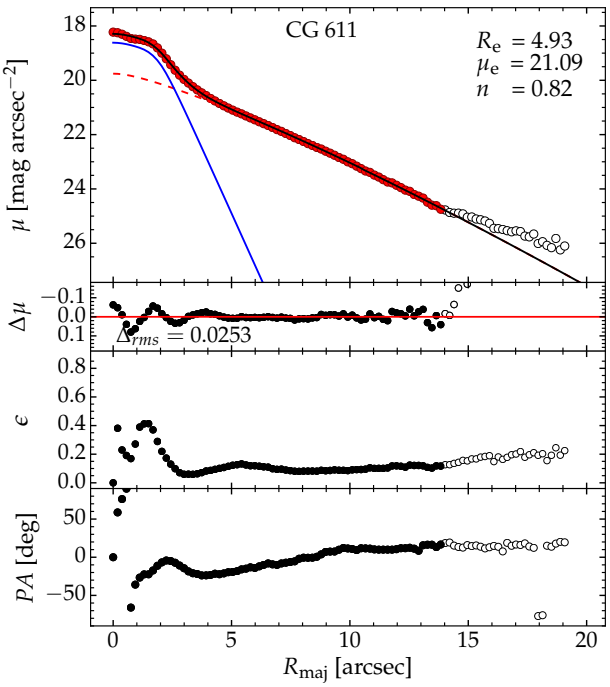

Figure 3. Upper panel: the observed (i.e. uncorrected for Galactic Extinction, redshift dimming, and K-correction) major-axis $CFHT$ r-band surface brightness profile of CG 611. The Sérsic (red) plus inner truncated disk (blue) model components have been convolved with the PSF. The best-fitting Sérsic parameters (prior to convolution with the PSF) are inset in the figure. The quantity $\Delta_{rms} = \sqrt{\sum_{i=1,N}(\text{data}_i - \text{model}_i)^2/(N-\nu)}$, where N is the number of data points used (filled circles) and ν is the number of model parameters involved in the fit. The middle panel shows the isophotal ellipticity profile $\epsilon = 1 - b/a$, where b/a is the ratio of the minor-to-major axis of the isophotes, while the lower panel shows the position angle of the isophote's major axis. The open circles beyond $\sim$14″ have been excluded from the fit, but an additional outer component could be added. See section 2.2.2 for more details. For reference, the major-axis half-light radius reported by SDSS for this galaxy is 3″.2.

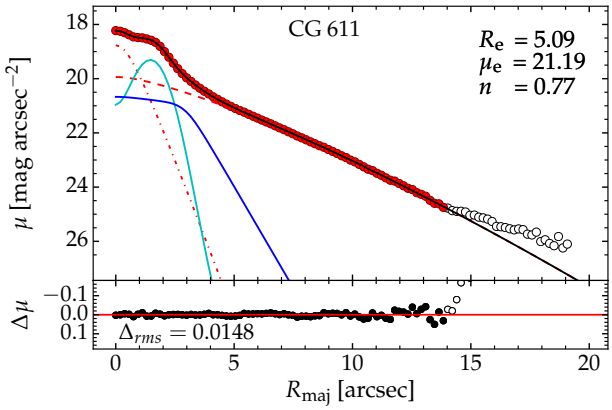

Figure 4. Building on Figure 3, a Gaussian function (cyan) has been added for the spiral arms/ring and a Sérsic function (dash-dotted red curve) for the inner barlens. The Sérsic parameters inset in this panel pertain to the outermost dashed red profile.

"ellicular" galaxy to an S0 lenticular galaxy or a spiral galaxy. On the other hand, if the galaxy loses its gas and dust, then it will immediately resemble dwarf ETGs in clusters. Therefore, in this manner, CG 611 appears similar to the transition-type dwarf galaxies mentioned by Grebel et al. (2003).

2.2.2. *Light profile*

After careful sky-subtraction and masking of interlopers, we used the new `IRAF` task ISOFIT (Ciambur 2015) to quantify the shape of the isophotes and extract the surface brightness profile and associated isophotal profiles (e.g. ellipticity, position angle, B_4, etc.) that describe the 2D distribution of the light. The surface brightness profile was then modeled with galactic components using the PROFILER software (Ciambur 2017).

We conducted our investigation from two stand points. First, we considered CG 611 to be dominated by a triaxial spheroid beyond $\approx 4''$, using the Sérsic model to match the bulk of the galaxy light. Second, we assumed that this light instead comes from a thick disk, using an exponential model instead.

Along the major-axis, from $\approx 4''$ to $14''$, the curvature of the light profile is described well with a Sérsic index equal to 0.82±0.05 (see Figure 3). It is perhaps worth noting the obvious, that this is different to the exponential value of 1 used for disks (Patterson 1940; de Vaucouleurs 1957; Freeman 1970; Elmegreen & Struck 2016, and references therein). The half-light radius of this component is 5.1±0.5 arcsec, equal to 1.1 kpc, which is typical for dwarf ETGs (e.g. Graham et al. 2006, their Figure 1b). Beyond $14''$, the surface brightness profile starts to fall away less sharply and the ellipticity profile slowly rises. This behavior is also present in the SDSS images and remains when the small 1-sigma uncertainty on the sky-background flux is subtracted from the light-profile, which has itself already had the sky-background flux subtracted from it. While we refrain here from adding an additional component, such as an exponential, we will return to this feature in the Discussion section.

At small radii, a truncated disk model (van der Kruit 1987; Pohlen et al. 2004) has been used to collectively account for the inner excess of light where a bulge-like feature (possibly a barlens: Laurikainen et al. 2011), a bar, and a spiral pattern reside. The truncation of this disk may be more dramatic than shown in Figure 3, but a sudden 'cliff-like' truncation produced similar overall results while producing an artificial local feature in the residuals. A non-truncated disk model did not work.

Rather than leave the decomposition at this stage, we went on to account for the spiral arms — which look a little like lopsided ansae or a partial ring — by using a Gaussian function for the associated bump in the light profile. The presence of these spiral arms shows up clearly in the ellipticity profile (see the middle panel of Figure 3), as does the additional bulge-like component, which we modeled with a Sérsic function. As noted, this bulge-like component may be a barlens, and the mismatch in position angle between it and the bar (see the lower panel of Figure 3) is a common feature of bars and their inner lenses. The result of fitting four components (spiral arms, barlens, truncated intermediate-scale disk, and large-scale Sérsic component) can be seen in Figure 4. The faint bar has effectively been subsumed into the truncated disk and inner bulge/barlens.

The combined apparent magnitude of the above four components, when independently fit to the inner $13''$ of the geometrical-mean axis (roughly $14''$ on the ma-

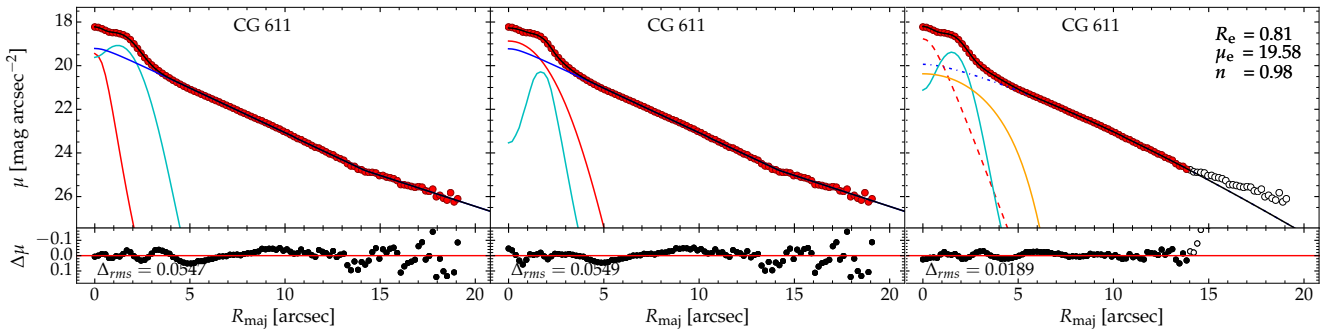

Figure 5. Left panel: an anti-truncated exponential disk model (blue curve: with transition at ∼14″ and inner/outer scalelength equal to $2''.7 \pm 0.1/3''.8 \pm 0.4$), plus a Gaussian function (cyan) for the spiral arms that form a partial ring, and a Sérsic function (red) for the inner bulge-like feature that may be a barlens. Middle panel: an alternate fit reveals a degeneracy and thus uncertainty with the previous decomposition whose innermost component (Sérsic function) was not bright enough to explain the central peak in the ellipticity profile (Figure 3). Right panel: including a Ferrers bar (orange) with the previous components did not help until we truncated the data at 14″ and replaced the anti-truncated disk with the Sérsic disk shown here by the dotted-dashed blue curve. The Sérsic parameters inset in this panel pertain to the innermost dashed red profile. Due to the differing radial extent of data, the value of Δ_{rms} in this panel should be compared to that in Figure 4, rather than that in the left and middle panels shown here.

jor axis), and integrated to infinity, is 14.95 mag. This magnitude is prior to any of the standard corrections[13]. As noted previously, the similarly uncorrected SDSS Petrosian r'-band apparent magnitude is 14.73 mag (AB). The reason that this is slightly (0.22 mag) brighter is most likely because of the excess light beyond ∼14″ that we have not accounted for with our model. The flux ratio of the main Sérsic component to all four components is 0.81.

We next explored the possibility that CG 611 is comprised of a large-scale disk rather than a spheroid. If it is, then this would remove the need for the inner disk shown in Figure 4 because the spiral arms, bar, and barlens could instead be features of the large-scale disk. Such a fit is somewhat akin to that used for blue compact dwarf (BCD) galaxies (e.g. Sandage & Binggeli 1984; Mrk 36 in Cairós et al. 2001a, or Mrk 370 in Cairós et al. 2002), although the color maps of BCDs (e.g. Cairós et al. 2001b) reveal a tendency for irregular off-center star-formation, unlike that seen in CG 611 (Figure 2).[14] Given the existence of anti-truncated disks, whose surface brightness profiles display an upward bend at large radii (e.g. Erwin, Beckman & Pohlen 2005), we have employed such a double exponential profile to represent the supposed disk. However, we could have used a single exponential function and continued to truncate the data at 14 arcsec, as done in Figures 3 and Fig4.

The left and middle panels of Figure 5 reveal a degeneracy that arose between the two inner components: the barlens and the spiral arms. Given the two peaks over the inner (< 3″) ellipticity profile, neither of these two fits appear satisfactory. We attempted adding an additional bar component, but without success. Potentially, the dust in this galaxy may have altered the image to yield a non-exponential disk out to 14″. Allowing for this possibility by using the Sérsic function to represent the disk within 14″, we still encountered this degeneracy with our three component fit (barlens, spiral arms, Sérsic-disk). However, we were able to overcome this when we subsequently included a Ferrers bar (Ferrers 1877; Sellwood & Wilkinson 1993), as seen in the right-hand panel of Figure 5. This is basically the solution obtained in Figure 4, but now interpreted differently. The radial extent of the Ferrers bar beyond the Gaussian function may indicate that the spiral arms are not fully captured by the Gaussian function. Use of an anti-truncated Sérsic disk — whose outer extent could be exponential in nature — would capture the full radial extent of the data. However, as far as we are aware, implementation of such a function has never been performed, and it is not necessary for our purposes.

At this point, we conclude that the main body of CG 611 is probably a triaxial spheroid but may be a thick disk without spiral structure. In the Discussion section, we compare CG 611 with other galaxies to see what insight we may gain.

2.3. *Spectroscopic Data*

The Echellette Spectrograph and Imager (ESI: Sheinis et al. 2000) on Keck II was used on the 10th evening of January 2016 as a part of Project W138E (PI: Graham), and on the 13th evening of March 2016 as a part of Project W028E (PI: Graham). To achieve our desired spectral resolution of ∼20 km s^{-1} for the velocity dispersion, we used the 0″.75 wide (and 20″ long) slit which gives an $FWHM$ spectral resolution of 55.9 km s^{-1}. Therefore, with a good ratio of signal-to-noise (S/N) we are able to measure velocity dispersion σ down to $FWHM/2.35 \approx 24$ km s^{-1} (see Janz et al. 2017, and their Figure 5, for further details).

We oriented the slit along the major-axis of the inner isophotes (P.A.=158° east-of-north). The combined exposures, under 0″.8 seeing, totaled 75 minutes. The wide wavelength coverage of ESI, from ∼4000 Å to ∼10,000 Å provides several spectral features to extract the velocity dispersion, including the calcium triplet (CaT), Mg, Fe, and Hα lines. To obtain the kinematical measurements of the stars, we averaged the values (weighted with the inverse variance squared) obtained from fits to the Mgb and Ca II triplet regions. The S/N ratio is >30 per Angstrom in the center for both spectral regions and around ∼6-7

[13] Galactic extinction, redshift dimming, K-correction, and dust-inclination correction.

[14] We are not ruling out potential evolutionary connections with BCDs (e.g. Caon et al. 2005), but rather remarking that CG 611 does not presently look like a BCD.

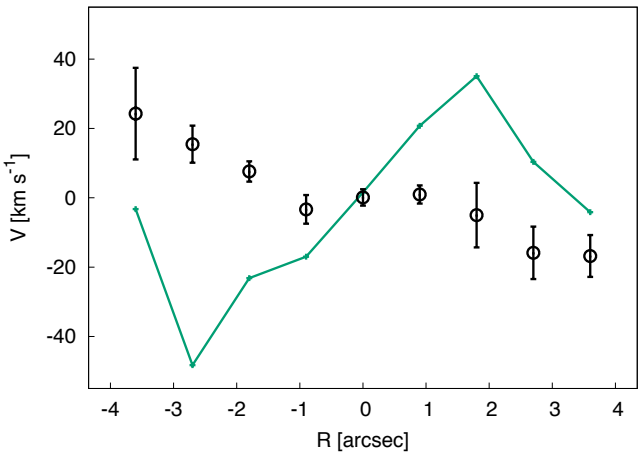

Figure 6. Observed rotation curve of the stars (open symbols) rises to ≈18 km s^{-1} by 1 $R_{\rm e,gal}$ (= 3″.2, = 0.71 kpc). The inner three data points additionally display evidence for a kinematically distinct core (KDC) in the form of mild counter rotation. The rotation curve of the gas (green curve) also counter rotates with respect to the luminosity-weighted stellar rotation within ≈1.3 $R_{\rm e,gal}$. Positive velocities mean a receding motion, and negative radii correspond to the S/SE direction (the lower right in Figure 1).

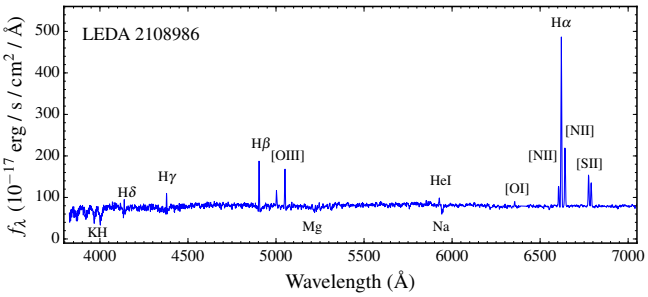

Figure 7. SDSS spectrum of LEDA 2108986 (CG 611) with notable emission and absorption lines marked.

for the largest radii. Radial velocities and velocity dispersions were measured using the penalized PiXel Fitting (pPXF) software by Cappellari & Emsellem (2004) and suitably matched template stars.

2.3.1. *Kinematics*

We measure a heliocentric recessional velocity of 2546±4 km s^{-1} from the stellar absorption lines, in good agreement with the SDSS value of 2562 ± 28 km s^{-1}. We measure a central stellar velocity dispersion $\sigma_{\rm cen} = 37 \pm 2$ km s^{-1} (see Janz et al. 2017 for further information). This value is greater than the spectral resolution limit of ∼24 km s^{-1} noted in the previous section, and is therefore a robust measurement rather than a lower limit.

Figure 6 reveals that the galaxy's stars rotate fairly symmetrically over the inner 3″.6 (0.80 kpc, 1.1 $R_{\rm e,gal}$). The positive stellar rotation (the left half of Figure 6) corresponds to the southern spiral arm in Figure 1. As can be seen in Figure 3, this radial extent of 4″.2 also happens to roughly correspond with the region where the disk (including the spiral arms) contributes to the light profile above that of the main Sérsic component. The stellar rotation at 1 $R_{\rm e,gal}$ is ≈18 km s^{-1} without correcting for the inclination of the disk. Based on the minor-to-major axis ratio of ∼0.90 at 1 $R_{\rm e,gal}$ (see Figure 3), this would correspond to an intrinsically round disk's inclination of ∼26 degrees; implying that the full rotational speed is ≈41 km s^{-1} in the plane of the disk.

The galaxy is additionally known to have several emission lines (see Figure 7). Fitting these independently in our Keck/ESI data with the pPXF software reveals the ionized gas dynamics, which is counter-rotating with respect to (most of) the stars within ≈1 $R_{\rm e,gal}$ (Figure 6). Such retrograde motion in barred galaxies has long been observed (e.g. Galletta 1987; Corsini 2014). With a peak gas rotation of −48 km s^{-1} at −2″.7 ($-0.84R_{\rm e}$) and +32 km s^{-1} at +1.″8 ($+0.6R_{\rm e}$), this gives a $V_{\rm gas}/\sigma_{\rm cen}$ ratio of around −1. These peaks roughly occur at the peak density of the stellar spiral arms.

There is additionally tentative evidence for a kinematically distinct component (KDC) in the form of a counter-rotating stellar core involving the inner ∼0.8 to ∼1.6 arcseconds (0.25 to 0.5 $R_{\rm e,gal}$). This roughly corresponds with the radial extent of the barlens and the faint bar, respectively. The amplitude of the counter rotation is marginal, at just a few km s^{-1}, although this feature is of course diluted by the signal coming from all the other stars along the same lines of sight through the galaxy. Amplitudes of counter rotation in other dwarf ETGs are also observed to be low, at around ∼5 km s^{-1} (Geha et al. 2003). It is possible that some new stars may have formed out of the accreted gas, which could explain this slight KDC. This would imply that yet another component should be added to the decomposition of the light profile in Figures 4 and 5. However, doing so would result in too much degeneracy and is therefore left for when higher spatial resolution imaging data becomes available.

3. DISCUSSION

3.1. *CG 611*

Given that CG 611 lives in a void, it is obviously not a late-type spiral galaxy that has been morphologically transformed by a cluster environment or a nearby massive galaxy — the argument often advocated for the creation of rotating dwarf early-type galaxies. CG 611 is also not hurtling through space at high speed, perhaps ejected from some distant galaxy cluster (e.g. Gill et al. 2005; Chilingarian & Zolotukhin 2015), because it is too far from any cluster, and if it were moving at high speed, then it would not have accreted its counter rotating gas disk.

As noted in Section 2.2.2, CG 611 possibly consists of an intermediate-scale stellar disk embedded within a much larger spheroid (see Savorgnan & Graham 2016b for other examples of such ES galaxies). Ann, Seo & Ha (2015) reclassified CG 611 from E/S0 to SA0/a; most likely because they detected the faint bar and the weak spiral structure from their visual inspection. However, relative to the S0 galaxy type, they shifted CG 611 slightly toward the late-type classification "Sa". It might be appropriate to shift it slightly toward the elliptical galaxy classification by recognizing it as an ES galaxy (see Figure 7 in Graham et al. 2016) in which CG 611 does not have a large-scale disk that dominates at large radii. That is, CG 611 may not be a disk galaxy with an inner bulge component, but instead an elliptical galaxy with an inner disk component.

Koleva et al. (2009, and references therein) report that

dwarf ETGs in clusters and groups are, in general, dominated (in stellar mass) by old stars, which are "likely coeval with that of massive ellipticals or bulges, but the star formation efficiency is lower". Due to additional intermediate-age (1-5 Gyr) populations and tails of ongoing star formation, their inner regions have (single-stellar-population)-equivalent ages of 1 to 6 Gyr. Ryś et al. (2015) also report that star formation within the last 5 Gyr is common in dwarf ETGs. They have interpreted this as support for the formation scenario in which tidal harassment drives gas (not stripped due to the ram pressure of the cluster/group hot X-ray gas) inward and induces a star formation episode. However, CG 611 is evidence that this scenario need not necessarily be true, or rather is not the only mechanism to account for intermediate-age cores in dwarf ETGs. This is because the external accretion of gas may have, in part, built its young nuclear region. The observation that a lower fraction of ordinary ETGs in clusters, than compared to isolated ETGs, are blue and star-forming (Lacerna et al. 2016, see also Collobert et al. 2006) reflects this and reveals a greater abundance of cold molecular gas in the field galaxies (see also Moorman et al. 2016).

Accretion of gas in CG 611 is apparent from the counter rotation of the gas relative to most of the stars, and from the non-symmetrical nature of the gas rotation curve about the photometric center of the galaxy (Figure 6). Ionized gas kinematics from future IFU data may help to establish when the gas in CG 611 was accreted; for example, offset rotation implies that it was acquired recently. We do not know the kinematic position angle of the ionized gas. An offset from the stars by ∼0 or ∼180 degrees implies dynamical equilibrium with the stars, and that the gas could have been in the galaxy for some time, while offsets greater than 30 degrees would suggest more recent accretion events. It would also be interesting to know if there is a bigger neutral hydrogen cloud around CG 611, as we only see the ionized gas that has been photoionized by the hot blue stars in the spiral arms. Curiously, the small spiral arms in CG 611 bare an uncanny resemblance to the nuclear spiral structure established in circumbinary disks around binary stars with co-rotating orbits (Diego Pinto et al., in preparation). Rather than two planets, the two over-densities at the ends of the bar give rise to the trailing spirals.

CG 611 has marginal evidence for a kinematically distinct *stellar* core (KDC) of ∼220–350 pc in diameter. KDCs have been observed in dwarf ETGs before, and Toloba et al. 2014 report on a 140 pc and 330 pc (in radius) KDC in the Virgo cluster galaxies VCC 1183 and VCC 1453. Penny et al. (2016, see their Figure 8) report on two dwarf ETGs with 1-1.5 kpc KDCs. Morphological peculiarities are common to isolated ETGs (Reda et al. 2004) and are therefore not an identifying signature of galaxy harassment or tidal stirring in cluster ETGs.

Far from being unusual, the majority of isolated lenticular galaxies contain ionized gas disks, and half of those disks rotate in the opposite sense to the stellar disk (Katkov et al. 2014, 2015). As Katkov et al. (2015) remark, this is expected if all of the gas is acquired by accretion of gas-rich satellites, or perhaps filaments of cold gas. For similar results, see Davis et al. (2011), Alatalo et al. (2013), Lagos et al. (2015), and also Jin et al. (2016) in regard to the MaNGA (Mapping Nearby Galaxies at Apache Point Observatory, Bundy et al. 2015) integral field spectroscopic survey. The Sydney-AAO Multi-object Integral field spectrograph (SAMI) Galaxy Survey (Croom et al. 2012; Bryant et al. 2015) has also found that $> 40\%$ of $z < 0.1$ ETGs outside of clusters have evidence for recently accreted gas (J. Bryant et al. in preparation). The rotation of this ionized gas displays misalignment with the stars motion and counter rotation. Such galaxy growth via disk growth likely accounts for the fate of many compact massive galaxies observed at high redshift; this is necessary to explain the abundance of compact massive spheroids in today's early-type galaxies (Graham 2013; Graham et al. 2015) and likely occurs quickly (see Papovich et al. 2016) so that their disks are suitably old by today.[15] Ordinary (i.e. non-dwarf) lenticular galaxies have long been known to contain old mass-weighted spheroids and younger disks (see section 4.3.3 of Graham 2013, and references therein) while the most massive ETGs — the giant elliptical galaxies — likely formed from major dry merger events in which their partially depleted cores were created through the damage of the ensuing supermassive black hole binary (Begelman et al. 1980; Merritt & Milosavljević 2005; Merritt 2006; Dullo & Graham 2014).

Finally, we comment on the previous observation that CG 611 follows the correlation between galaxy luminosity and galaxy Sérsic index for ETGs. Had CG 611 not grown its inner components, that is, if its surface brightness profile within the inner 14″ (∼3 kpc) was described by just the Sérsic component shown in Figure 3, then it would appear as a low-n (high-L) outlier in the L–n diagram. CG 611 would shift from $M_{g'} = -17.96$ mag and $n = 2.3$ (the single Sérsic fit from SDSS) to $M_{g'} = -17.7$ mag and $n = 0.8$, positioning it rather close to VCC 9 (IC 3019) in Figure 10 of Graham & Guzmán (2003). This therefore offers a potential explanation for why VCC 9 is an outlier in this diagram — it may not have accreted sufficient material at its core to increase its galaxy Sérsic index. CG 611 additionally raises the question as to whether or not past bulge/disk decompositions have got the bulge and disk components around the right way. For example, the interesting compact elliptical galaxy LEDA 3090323, with an AGN and suspected $\sim 2 \times 10^6$ $M_\odot$ black hole (Paudel et al. 2016a), may be worth exploring further in this regard.

3.2. *Other galaxies*

It is relevant to ask if CG 611 is unique in appearance, or instead similar to other known galaxies. Disk features and faint spiral structures have indeed been reported in dwarf ETGs before (Jerjen et al. 2000; Barazza et al. 2002; Graham & Guzmán 2003; Graham et al. 2003; Lisker et al. 2006; Lisker & Fuchs 2009; Janz et al. 2012; Penny et al. 2014). Perhaps of particular relevance is the "Emerald Cut" galaxy (LEDA 074886: Graham et al. 2012), a dwarf ETG with an intermediate-scale disk seen edge-on. In that galaxy, the disk rotates at 33±10 km s^{-1}, compared to our estimated edge-on rotation of ≈41 km s^{-1} for CG 611. LEDA 074886, and in particular its isophotes, illustrates well how the disk is confined to within the galaxy. CG 611 *may* be something of a face-on

[15] Less massive ES and S0 galaxies have younger disks than their more massive brethren.

analog to LEDA 074886. It can, however, be challenging to obtain kinematic data at large radii to reveal the kinematic decline of disks in dwarf galaxies. Although, this has been achieved for non-dwarf ES galaxies with intermediate-scale disks, e.g. NGC 3115 and NGC 3377 (Arnold et al. 2011, 2014).

As to other dwarf ETGs displaying more face-on disks than LEDA 074886, the inner spiral structure in CG 611 is very similar to the Virgo cluster dwarf ETGs VCC 216 and VCC 490 (see Figure 2 from Lisker et al. 2009 which displays these galaxies and their unsharp masks). NGC 4150, a member of a sparse group, additionally resembles CG 611. We have therefore discovered that the cluster and group environment are *not* required for creating these dwarf ETGs. The residual image (data minus symmetric model) of the "compact elliptical" galaxy J094729.24+141245.3 in Huxor et al. (2013) also appears to show tentative evidence for an inner spiral structure similar to that seen in CG 611. While those authors argued that there was no underlying disk in J094729.24+141245.3, if this spiral pattern is confirmed — with say *Hubble Space Telescope* imaging — then this galaxy may likely also contain an intermediate-scale disk. In passing, we note that the compact galaxy LEDA 083546 (Paudel et al. 2016b) also possesses several similarities to CG 611.

Below, we focus on two galaxies resembling CG 611, but that have been treated rather differently in the literature. This adds to the diagnostic dilemma we encountered in Section 2.2.2, in which it was not obvious whether CG 611 contains a large-scale disk or an intermediate-scale disk within a large-scale spheroid.

3.2.1. *NGC 2983*

The non-dwarf ETG NGC 2983 ($M_B \approx -20.5$ mag; $B-V \approx 0.9$) is remarkably similar to CG 611 in appearance, with the major-axis position angle of its "barlens" considerably rotated with respect to its bar (Laurikainen et al. 2011, their Figure 8; see also Bettoni et al. 1988). Like CG 611, NGC 2983 also contains short spiral arms at the ends of its bar. Bettoni et al. (1988) report on the presence of an additional, larger "lens" from ∼20 to ∼50 arcseconds (see their Figures 1c and 3)[16], which is evident in the Carnegie-Irvine Galaxy Survey (Ho et al. 2011) image[17] and is something of a broad, ring-like, annular extension of the spiral arms. This "lens" plus the outer regions of this galaxy are modeled with a single exponential disk by Laurikainen et al. (2010), who therefore treat this galaxy as an SB0. Given that the axis ratio beyond 50″ is around 0.57 in this galaxy, it is understandable why this was done. However, beyond the ∼20″-long bar, the rotation curve can be seen to decline (albeit only by 25%) as one starts to move outward through the "lens". Despite this, Bettoni et al. (1988) remark/assume that the structure beyond this is probably oblate with an intrinsic flattening of 0.25. This raises the question of whether CG 611 might consist of a large-scale disk hosting a small faint bar with a central barlens and short spiral arms coming off its ends, plus (perhaps) a larger "lens" or ring (see Buta & Crocker 1991) that extends the spiral arms out to 4–5 arcseconds. If so, then the bar component in the right-hand panel of Figure 5 might have extended out beyond the Gaussian component — used to represent the spiral arms/ring — because it was additionally capturing such a "lens".

[16] The 10″ scale-bar in their Figure 1 should read 20″.

[17] `https://cgs.obs.carnegiescience.edu`

3.2.2. *CGCG 036-042*

The r-band surface brightness profile of CG 611 (Figure 3) is also remarkably similar to that of the isolated[18], compact ETG CGCG 036-042 (Paudel et al. 2014, see their Figure 2). However, this galaxy is not presented as hosting a large-scale disk. Modeling the major-axis light profile of CGCG 036-042, Paudel et al. (2014) find that the best fit has an inner Sérsic component with $n = 1.06$, and an outer Sérsic component with $n = 0.78$ (compare our Figure 3). Furthermore, they report on an extended diffuse stellar component from ∼3 kpc out to 10 kpc. Beyond ∼3 kpc, we too observe an extended feature in the light profile of CG 611 that appears similar to the extended feature in CGCG 036-042. For simplicity, we chose not to model this outer feature in Figures 3 and 4, but it can be seen in the upturn of the ellipticity profile and the flattening of the position angle profile beyond 14″ (∼3 kpc) in Figure 3. Moreover, CGCG 036-042 has $M_r = -18.21$ mag (Paudel et al. 2014), comparable to the brightness of CG 611 ($M_r = -17.96$ mag).

The compact ETG CGCG 036-042 and the non-dwarf ETG NGC 2983 serve to illustrate that other galaxies, not just dwarf ETGs, which are similar in appearance or light profile to CG 611 exist, and that they have been modeled in different ways. This echoes the ambiguity seen in section 2.2.2, and motivates us to develop ways to resolve this issue for galaxies in the future. In particular, we introduce a diagnostic diagram in Section 3.3.2 to help address this.

3.3. *Implications*

3.3.1. *Theoretical insight/connections*

What does all this imply for the "galaxy harassment" model in clusters (Moore et al. 1996, 1998) and the related "tidal stirring" model, which can operate around massive galaxies (Mayer et al. 2001a, 2001b)? Both of these models result in late-type disk galaxies forming bars, and the remaining outer disk being stripped off. These two processes initially produce rather flat "naked bars", which under select (near face-on) viewing angles superficially look like ellipsoidal galaxies. Sufficient agitation can eventually turn these flat bars into triaxial spheroidal structures, and the Sagittarius dwarf galaxy may be a good example of this (Łokas et al. 2010). Stott et al. (2007) and D'Onofrio et al. (2015) present additional evidence for such transformations. While we do not deny that this process can occur, we have revealed that this is clearly not the origin of all dwarf ETGs; an observation that may have some support from De Lucia et al. (2009) who report on a deficit of post-starburst dwarf galaxies in two clusters.

In passing we note that the "tidal stirring" model applies to the metamorphosis of galaxy disks, and thus it is different from the tidal interaction models advocated for the creation of low-mass compact elliptical (cE) galaxies (King 1962; Rood 1965; Faber 1973; King & Kiser

[18] See Section 2.1 of Paudel et al. (2014).

1973; Keenan & Innanen 1975; Wirth & Gallagher 1984). These early models suggested that a massive companion galaxy stripped off the outer layers of a normal elliptical galaxy to create the relatively rare class of cE galaxies. Subsequent work has suggested that the original galaxy was instead a lenticular galaxy, and thus the cE galaxies are predominantly the bulges of former S0 galaxies (Bekki et al. 2001; Graham 2002), or the cE galaxies in isolation never grew a substantial disk in the first place (Graham 2013).

Although CG 611, and the other isolated dwarf ETGs presented in Janz et al. (2017), undermine the "Galaxy harassment" and "tidal stirring" models for the creation of *all* dwarf ETGs, those two mechanisms *might* preferentially act on lower mass, late-type spiral, and dwarf irregular galaxies, turning them into dwarf spheroidal (dSph) galaxies (Klimentowski et al. 2009; Kazantzidis et al. 2011, 2013; Paudel & Ree 2014) by removing much of their disk mass. These dSph galaxies (with $M_B \gtrsim -13$ to -14 mag) may then be somewhat different from the dwarf/ordinary ETG sequence at $M_B \lesssim -13$, with many of the most luminous ETGs ($M_B \lesssim -20.5$ mag) additionally displaying a departure in the luminosity–(central surface brightness) diagram due to their partially depleted cores (Graham & Guzmán 2003). Some of the dSph galaxies would then be more connected with low-mass late-type, dwarf Irregular, and "transition type" dwarf galaxies (e.g. Grebel et al. 2003) and likely show different behaviors in certain scaling diagrams. Indeed, the color–magnitude diagram for ETGs already suggests that there is a difference at $M_B \sim -13$ to -14 mag (e.g. Penny & Conselice 2008). Roediger et al. (2016) note that quenching of these low-mass ETGs may have occurred in groups and smaller host halos prior to entering the cluster environment. Although, it should be remembered that dwarf spheroidal (dSph: $M_B \gtrsim -13$ mag) galaxies can also evolve in isolation (Makarova et al. 2016), and thus this process is not a requirement. Furthermore, Smith et al. (2015, see also Smith et al. 2010 and Bialas et al. 2015) ran a suite of numerical simulations and found that harassment of low-mass disk galaxies was only effective if they plunged deep into the dense core of a galaxy cluster. They found that less than one-quarter of orbits from a cosmological simulation resulted in any stripping of disk stars, as required in the harassment scenario. In addition, Aguerri (2016) concluded, based on his analysis of the $(R_{\rm e,bulge}/h_{\rm disk})$–$n$ diagram, that most dwarf ETGs in clusters are not transformed disk galaxies.

In CG 611, minor mergers may have brought in some gas and stars in a clumpy manner, which is known to lead to the growth of disks, including counter rotating cores and halos (Sancisi et al. 2008; González-Samaniego et al. 2014; Lane et al. 2015; Christensen[19] et al. 2016). As noted by Genel et al. (2010), minor mergers and smooth accretion, rather than major mergers, dominate galaxy growth (see also Murali et al. 2002; Semelin & Combes 2005; Maller et al. 2006), and this supply channel also favors the formation of disks. Smooth gas flow onto a galaxy can occur via spherical accretion of $\sim 10^4$–10^5 K halo gas (e.g. White & Frenk 1991, see their Section 7; Birnboim & Dekel 2003) or more directly from unshocked cold streams (e.g. Kereš et al. 2005; Dekel & Birnboim 2006; Brooks et al. 2009; Dekel et al. 2009; Cornuault et al. 2016). This cold mode of delivery may be the most efficient of the mechanisms (Genel et al. 2010; van de Voort et al. 2011; Lu et al. 2011) and Pichon et al. (2011) have revealed how these cold gas streams can build a disk in a coherent planar manner (see also Danovich et al. 2012, 2014; Prieto et al. 2013; and Stewart et al. 2013).

Examining the kinematics of a larger sample of isolated dwarf ETGs will enable one to compare their properties with cluster dwarf ETGs and in so doing learn about their collective origin. For example, Paudel et al. (2010) have suggested that old metal poor dwarf ETGs found in the central high-density regions of clusters may have formed along with the cluster while the younger more metal rich dwarf ETGs (which tend to have disk features) have fallen in at a later time. While plausible, the assumption that the infalling galaxies were disk galaxies that underwent a structural transformation may need revising if isolated dwarf ETGs already have the same structural and kinematic properties as this cluster population. CG 611 is one such galaxy that suggests they do, and Janz et al. (2017) presents a further eight such galaxies.

A related issue is the dominance at low masses of dwarf ETGs in clusters and the prevalence of (higher mass) Scd-Im galaxies in the field. Although we do not answer this question, obviously past claims that have attempted to answer this solely in terms of harassment and transformation of late-type galaxies need to be reconsidered, because dwarf ETGs similar to those in clusters are now known to also exist in the field. There is a formation channel for dwarf ETGs that does not involve the harassment of disk galaxies. In the Λ cold dark matter (ΛCDM) model of galaxy formation, low-mass dwarf galaxies naturally form, and help to build up bigger galaxies. One can speculate that these small systems might have preferentially formed in over-dense regions that later became galaxy groups and clusters. That is, they may have effectively formed as ETGs rather than as late-type galaxies that were subsequently relocated and transformed.

3.3.2. *Spin–ellipticity diagrams*

We have seen in Section 2.2.2 that CG 611 may have an intermediate-scale disk, and we have learned in section 3.2 that other galaxies certainly do. Here we propose a revision to a popular diagram, used to characterize the kinematic behavior of ETGs as either 'fast rotators' or "slow rotators", by displaying additional information helpful for identifying galaxies with intermediate-scale disks. A key ingredient is kinematic information extending beyond the radial extent of a galaxy's disk. While we do not yet have this information for CG 611, it exists for other galaxies with intermediate-scale disks and should become available for many more galaxies through present and upcoming 'integral field unit' spectroscopic surveys such as SAMI (Croom et al. 2012; Fogarty et al. 2015).

Measuring the rotation over roughly the inner 0.5–1.0 half-light galaxy radii, $R_{\rm e,gal}$, of 260 ETGs, the ATLAS^{3D} team realized that many galaxies classified as elliptical had been misclassified because they rotated fast; they contained disks (Emsellem et al. 2011; Krajnović et al. 2013). Simply looking at images, and with-

[19] https://www.youtube.com/watch?v=_Ssc1GsqHds

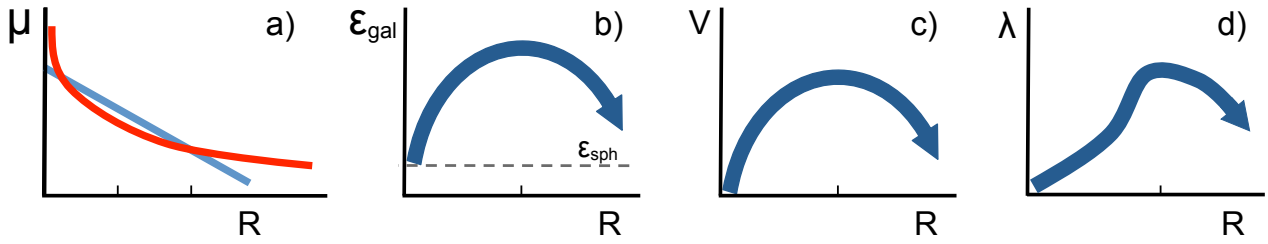

Figure 8. Panel a) shows the surface brightness profile of an "ES" galaxy with a Sérsic spheroid component (red) and an exponential intermediate-scale disk component (blue). Unlike large-scale disks in S0 galaxies, intermediate-scale disks do not dominate the flux at large radii. Panels b, c and d) roughly show how the ellipticity, rotational velocity, and angular momentum profiles would behave.

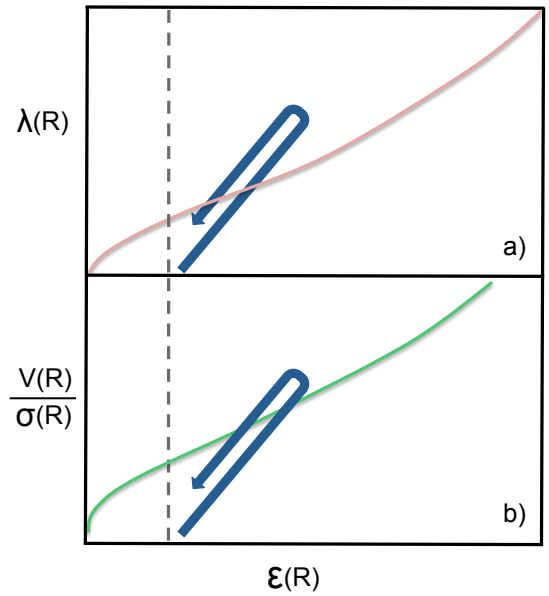

Figure 9. Blue tracks show how a galaxy with an intermediate-scale disk might move as one samples the local angular momentum, λ, and the local rotational velocity (calibrated against the local or central velocity dispersion) as a function of increasing radius. The dashed line denotes some fixed ellipticity for the spheroidal component of the galaxy, as shown in Figure 8. Panel a): the pink curve approximates the edge-on view for ellipsoidal galaxies shown in Emsellem et al. (2007, their Fig.3), although this curve pertains to a luminosity-weighted spin parameter integrated within a radius of more than $\sim 1R_e$ and assumes an orbital anisotropy $\beta = 0.70 \times \epsilon$. Panel b): the edge-on isotropic model from Cappellari et al. (2007, their Figure 3) is approximated here by the green curve.

out a careful bulge/disk/etc. decomposition of the galaxy light, it is easy to appreciate why many ES and S0 galaxies have been misclassified as E galaxies. The ATLAS^{3D} team therefore continued to use the earlier classification (Emsellem et al. 2007; Cappellari et al. 2007) of "fast rotator" (FR) and "slow rotator" (SR) to replace the photometrically determined S0 and E classification. The limitation with this new two-family dichotomy is that, while all ETG galaxies could previously be accommodated for through the continuum from E to ES to S0, the ES galaxies with intermediate-scale disks are not so adequately accounted for with the FR/SR typing based on the kinematics within $1R_e$. The issue is that these somewhat overlooked galaxies are fast rotators at small to intermediate radii and slow rotators at large radii.

To parameterize, and thus better understand galaxies, Emsellem et al. (2011) replaced the luminosity-weighted $(V/\sigma)_e$–ϵ_e diagram (Emsellem et al. 2007) with the luminosity-weighted λ_e–ϵ_e diagram. The quantities involved, computed within the galaxy effective half light radius (hence the subscripts 'e'), are rotational velocity (V), velocity dispersion (σ), isophotal ellipticity (ϵ), and a 'spin' parameter defined as

$$\lambda_R = \frac{\sum_{i=1}^{N_p} F_i R_i |V_i|}{\sum_{i=1}^{N_p} F_i R_i \sqrt{V_i^2 + \sigma_i^2}}, \quad (1)$$

with F_i and R_i the flux within, and geometric-mean radius of, the central then annular spatial bins out to some final radius R. Romanowsky & Fall (2012) suggested replacing $\lambda_e \equiv \lambda_{R=R_e}$ with the specific angular momenta, $j_* = J_*/M_*$, where J_* is the total angular momentum and M_* is the total stellar mass (Fall 1983; Casuso & Beckman 2015, and references therein). While there are benefits to a more global parameter, instead of a central ($R < 1R_e$) parameter, especially given that most of the angular momenta can be at large radii, we propose and advocate capturing more information than a single parameter like λ_e or j_* or ϵ.

Galaxies have been placed into a diagram of spin, λ_e, versus a single ellipticity parameter, ϵ, and a dividing line used to type them as FR or SR (e.g. Emsellem et al. 2011). However, λ is a function of radius, and we suggest that this diagram not plot galaxies as points, but instead plot them as tracks. Sampling a galaxy at many radii can result in a track across this diagram. Toloba et al. (2015) begin to demonstrate this in the dwarf regime by showing results at $0.5R_e$ and $1R_e$. This is important because the ES galaxies, but not the S0 galaxies, will transition from the FR region into the SR region of the diagram as one starts to sample beyond the radial extent of their intermediate-scale disk.

Weighted by all the data within some radius R, the *cumulative* stellar spin parameter λ_R given above is less sensitive than the *local* stellar spin parameter $\lambda(R)$ computed within an elliptical annulus of radius R (see Foster et al. 2016; Bellstedt et al. 2017a). As such, radial profiles of $\lambda(R)$ can be more revealing than radial profiles of λ_R. In addition, radial profiles of ellipticity are far more informative than a single luminosity-weighted value within some radius.

Building on Liller (1966), Figure 8 reveals what a galaxy with a somewhat edge-on intermediate-scale disk

may look like in radial plots of a) surface brightness, b) ellipticity, c) velocity (or velocity divided by the central velocity dispersion), and d) the local spin parameter. Figure 9 shows how such a galaxy would move through the spin–ellipticity diagram as a function of increasing galaxy radius.

We advocate that galaxies should not be treated as single points in a stationary λ_{R_e}–ϵ_e diagram, but instead be treated as tracks moving across the $\lambda(R)$–$\epsilon(R)$ diagram. Given the shift to IFU surveys in recent years, this information can be readily extracted. Similarly, individual galaxy tracks in the $V(R)/\sigma(R)$–$\epsilon(R)$ diagram (e.g. Busarello et al. 1988, their Figure 11) would be more informative than points. While E galaxies should not move much, and S0 galaxies will quickly reach a maximum, the ES galaxy tracks will be seen to recede from this maximum as one probes out to larger radii. The use of 'tracks' would therefore aid in the identification of the often overlooked, and subsequently mistreated, ES galaxies. It would, for example, enable a fuller understanding of the ETGs in the Calar Alto Legacy Integral Field Area (CALIFA) survey (Sánchez et al. 2012). From that team's multi-component decomposition of the light from 127 ETGs, Méndez-Abreu et al. (2016) designated 36 of them as "B/BD" systems, that is, they could not decide if these galaxies were either a pure bulge or a bulge+disk system. Many of these may be ellicular (ES) galaxies. Excitingly, many of their galaxies have kinematic data out to several effective radii (e.g. Falcón-Barroso et al. 2016), as does data from SAMI (Croom et al. 2012; Fogarty et al. 2015) and MaNGA (Bundy et al. 2015), enabling an exploration of fledgling disks and the transformation of elliptical galaxies into lenticular galaxies.

Unfortunately, we do not have enough radial extent in our kinematic data for CG 611 to make an informative λ_{R_e}–ϵ_e diagram. This may be the situation for many dwarf galaxies due to their faint (and quickly declining) surface brightness profiles. However, we note that aside from dwarf ES (dES) galaxies, it will be interesting to see the movement of ordinary (brighter) ES galaxies in the $\lambda(R)$–$\epsilon(R)$ diagram. Such "disk ellipticals" have been identified in Liller (1966), Nieto et al. (1988), Simien & Michard (1990), Michard & Marchal (1993), and elsewhere. Specific recent examples include NGC 3412 (Erwin et al. 2005, their Figure 3a), NGC 3115 (Arnold et al. 2011) and NGC 3377 (Arnold et al. 2014). Other such galaxies of interest that have intermediate-scale disks, include: NGC 1271 (Graham et al. 2016); Mrk 1216 and NGC 1332 (Savorgnan & Graham 2016b); NGC 821, NGC 3377, and NGC 4697 (Savorgnan & Graham 2016a); and NGC 4473 (Foster et al. 2013; Alabi et al. 2015). Galaxies like NGC 1277 (Graham et al. 2016) and NGC 3115 (Savorgnan & Graham 2016b) also have disks fully embedded in their spheroids, but they extend quite far out and thus globular clusters or planetary nebula, rather than long-slit or integral field unit (IFU) spectroscopy will likely be required to sample the dynamics beyond the disk (e.g. Hui et al. 1995; Romanowsky et al. 2003; Teodorescu et al. 2005; Woodley et al. 2007; Pota et al. 2013; Brodie et al. 2014; Richtler et al. 2015; Toloba et al. 2016), though this will be challenging for CG 611 at a 'luminosity distance' of 46.7 Mpc.

3.3.3. S_K^2 *and the Fundamental Plane*

The existence of galaxies with varyingly sized disks raises a second issue that we address here.

To account for the contribution to kinetic energy coming from not just the random motion of stars, as traced by the velocity dispersion σ, but also from the ordered motion given by the rotational velocity $V_{\rm rot}$, Busarello et al. (1992) effectively used the quantity

$$S_{1/3}^2 \equiv \frac{3}{2}\sigma^2 + \frac{1}{2}V_{\rm rot}^2,$$

where $3\sigma^2$ represents the sum of the velocity dispersion squared in each plane

$$\sigma_{XY}^2 + \sigma_{XZ}^2 + \sigma_{YZ}^2. \quad (2)$$

The existence of orbital anisotropy means that these last three quantities may not be equal. The quantity $S_{1/3}^2$ reduces to $1.5\sigma^2$ if there is no rotation in a galaxy, and reduces to $0.5V_{\rm rot}^2$ if there is only a rotating disk with no velocity dispersion. The important 1 to 3 scaling reflects that rotation predominantly occurs in one plane while velocity dispersion occurs in all three planes.

The above quantity is generalized in Weiner et al. (2006), such that

$$S_K^2 \equiv \sigma^2 + KV_{\rm rot}^2,$$

which is equivalent to the first expression when $K = 1/3$. As can be seen, the quantity K sets the ratio between the ordered and random motions in this generalized kinematic scaling expression S_K^2.

It would appear logical that studies building on the "Fundamental Plane" (FP: Djorgovski & Davis 1987), which are now using $S_{1/2}^2$ rather than just σ^2 for the ETGs (and for spiral galaxies, e.g. Kassin et al. 2007; Zaritsky et al. 2008; Cortese et al. 2014), may benefit from a recognition of ES galaxies in their surveys and a modified treatment of them.

The virial theorem, considered to be the basis for the FP, relates the mass M of a system to the speeds and sizes of its components. At a galaxy component level,

$$M \approx \frac{3}{2}\sigma^2 R_{\rm sph} + \frac{1}{2}V_{\rm rot}^2 R_{\rm disk}. \quad (3)$$

For disk galaxies, the ratio of the spheroid's effective half-light radius to the disk's scalelength is known to be fairly constant, with $R_e/h \approx 0.2$ (e.g. Courteau et al. 1996; Graham & Worley 2008, and references therein). However, in ES galaxies, the size of the disk relative to the spheroid is not constant. Although many FP-type studies are now accounting for the different kinematics of the two major components in galaxies, i.e. spheroid and disk, they do not yet account for the different physical sizes of these components. This may be an issue for studies of ETGs including both S0 and ES galaxies. Rather than simply using, or implicitly assuming, a single galaxy size — typically the 'effective half-light radius' $R_{\rm e,gal}$ — the use of appropriate galaxy component sizes may help to bring increased physical meaning to the photometric and spectroscopic survey data. Doing so may lead to a deeper physical understanding of galaxies, possibly reduce some of the scatter about the modified Fundamental Plane,

and in turn lead to an improved distance indicator for studies of peculiar velocity flows.

4. CONCLUSIONS

CG 611 is a dwarf early-type galaxy that formed in isolation (nature, rather than nurture by a parent galaxy cluster or a neighboring 'big brother' galaxy). It has experienced gas accretion which contributed to the build-up of the inner disk. This ETG's ionized gas is observed to counter-rotate with respect to the majority of stars in the inner $\approx$1 $R_{\rm e,gal}$. Such a scenario is mentioned in Koleva et al. (2013), and it has resulted in the creation of this dwarf galaxy. CG 611's isolation, and accreted gas disk, reveals that it is not a late-type galaxy morphologically transformed by a cluster environment, i.e. the argument advocated for years for the creation of the rotating dwarf ETGs. If CG 611 were to fall into a cluster, ram pressure stripping would remove its gas and dust, and it would then immediately resemble the dwarf ETGs already in clusters.

Having taken the 'cluster environment' out of the equation, CG 611 reveals that it is accretion, the build-up of gas from the primordial supply, that can give dwarf ETGs their spin (e.g. Jin et al. 2016). That is, rotating dwarf ETGs are not necessarily built from the removal of material (from late-type galaxies) in a cluster — although some likely are.

To better understand the nature of CG 611, it would be helpful to: *i*) obtain an *HST* image, enabling one to quantify additional components near the center of this galaxy and better constrain the suspected intermediate-scale disk, bar and lens; *ii*) see what, if any, hydrogen or molecular gas cloud is associated with CG 611, as this should provide additional information about the disk formation in this galaxy; *iii*) acquire kinematical information at larger radii, perhaps by probing the globular cluster system, to determine the ratio of ordered rotation to random motion of the main galaxy beyond the inner $R_{\rm e,gal}$; and *iv*) check for any AGN X-ray emission coming from this galaxy, because it is a good candidate to host an intermediate mass black hole.

In several aspects, CG 611 resembles a number of other dwarf ETGs, in particular, VCC 216, VCC 490, and NGC 4150. In regards to two other possibly similar galaxies, it would be interesting to check for the existence of an inner spiral in the isolated compact elliptical galaxy J094729.24+141245.3 (Huxor et al. 2013). This galaxy may be an additional example of ETG evolution via disk growth rather than disk stripping. It will also be interesting to obtain spatially resolved kinematics for CGCG 036-042 (Paudel et al. 2014) with its 4 Gyr old inner exponential component, and thereby answer what rotation, if any, is associated with this component.

The disk in CG 611, which is undergoing development, has motivated us to advocate representing galaxies by tracks, rather than single points, in a revised spin–ellipticity diagram. Although we do not yet have sufficiently radially extended kinematics to do this for CG 611, Bellstedt et al. (2017b) presents such tracks for a number of brighter "disk elliptical" ES galaxies. We have additionally advocated the consideration of disk and spheroid sizes when using the disk and spheroid kinematics for the quantity $S_K = \sqrt{K\,V_{\rm rot}^2 + \sigma^2}$, which may prove useful for "Fundamental Plane" type studies.

This research was supported under the Australian Research Council's funding scheme (DP17012923), and through Swinburne's Keck time Project Codes W028E and W138E. This research has made use of the NASA/IPAC Extragalactic Database (NED), the SAO/NASA Astrophysics Data System, and the SDSS archives.

REFERENCES

Abazajian, K., Adelman-McCarthy, J. K., Agüeros, M. A., et al. 2005, AJ, 129, 1755
Aguerri, J. A. L. 2016, A&A, 587, A111
Alabi, A. B., Foster, C., Forbes, D. A., et al. 2015, MNRAS, 452, 2208
Alatalo, K., Davis, T. A., Bureau, M., et al. 2013, MNRAS, 432, 1796
Ann, H. B., Seo, M., & Ha, D. K. 2015, ApJS, 217, 27
Argudo-Fernández, M., Verley, S., Bergond, G., et al. 2015, A&A, 578, A110
Arnold, J. A., Romanowsky, A. J., Brodie, J. P., et al. 2011, ApJL, 736, L26
Arnold, J. A., Romanowsky, A. J., Brodie, J. P., et al. 2014, ApJ, 791, 80
Barazza, F. D., Binggeli, B., & Jerjen, H. 2002, A&A, 391, 823
Begelman, M. C., Blandford, R. D., & Rees, M. J. 1980, Nature, 287, 307
Bekki, K., Couch, W. J., Drinkwater, M. J., & Gregg, M. D. 2001, ApJL, 557, L39
Bellstedt, S., Forbes, D.A., Foster, C., et al. 2017a, MNRAS, 467, 4540
Bellstedt, S., Graham, A.W., Forbes, D.A., et al. 2017b, submitted
Bender, R., Burstein, D., & Faber, S. M. 1992, ApJ, 399, 462
Benson, A. J., Toloba, E., Mayer, L., Simon, J. D., & Guhathakurta, P. 2015, ApJ, 799, 171
Bettoni, D., Galletta, G., & Vallenari, A. 1988, A&A, 197, 69
Bialas, D., Lisker, T., Olczak, C., Spurzem, R., & Kotulla, R. 2015, A&A, 576, A103
Birnboim, Y., & Dekel, A. 2003, MNRAS, 345, 349
Blanton, M. R., Kazin, E., Muna, D., Weaver, B. A., & Price-Whelan, A. 2011, AJ, 142, 31
Boselli, A., Boissier, S., Cortese, L., & Gavazzi, G. 2008, ApJ, 674, 742
Boselli, A., Cuillandre, J. C., Fossati, M., et al. 2016, A&A, 587, A68
Brodie, J. P., Romanowsky, A. J., Strader, J., et al. 2014, ApJ, 796, 52
Brooks, A. M., Governato, F., Quinn, T., Brook, C. B., & Wadsley, J. 2009, ApJ, 694, 396
Bryant, J. J., Owers, M. S., Robotham, A. S. G., et al. 2015, MNRAS, 447, 2857
Bundy, K., Bershady, M. A., Law, D. R., et al. 2015, ApJ, 798, 7
Busarello, G., Filippi, S., & Ruffini, R. 1988, A&A, 197, 91
Busarello, G., Longo, G., & Feoli, A. 1992, A&A, 262, 52
Buta, R., & Crocker, D. A. 1991, AJ, 102, 1715
Butcher, H., & Oemler, A., Jr. 1978, ApJ, 226, 559
Cairós, L. M., Vílchez, J. M., González Pérez, J. N., Iglesias-Páramo, J., & Caon, N. 2001a, ApJS, 133, 321
Cairós, L. M., Caon, N., Vílchez, J. M., González-Pérez, J. N., & Muñoz-Tuñón, C. 2001b, ApJS, 136, 393
Cairós, L. M., Caon, N., García-Lorenzo, B., Vílchez, J. M., & Muñoz-Tuñón, C. 2002, ApJ, 577, 164
Caon, N., Cairós, L. M., Aguerri, J. A. L., & Muñoz-Tuñón, C. 2005, ApJS, 157, 218
Cappellari, M., & Emsellem, E. 2004, PASP, 116, 138
Cappellari, M., Emsellem, E., Bacon, R., et al. 2007, MNRAS, 379, 418
Casuso, E., & Beckman, J. E. 2015, MNRAS, 449, 2910
Chilingarian, I., Cayatte, V., Revaz, Y., et al. 2009, Science, 326, 1379
Chilingarian, I., & Zolotukhin, I. 2015, Science, 348, 418
Chilingarian, I. V., Zolotukhin, I., Katkov, I., Melchior, A.-L. 2017, ApJS, 228, 14

Christensen, C. R., Davé, R., Governato, F., et al. 2016, ApJ, 824, 57
Ciambur, B. C. 2015, ApJ, 810, 120
Ciambur, B. C. 2017, PASA, 33, 62
Collobert, M., Sarzi, M., Davies, R. L., Kuntschner, H., & Colless, M. 2006, MNRAS, 370, 1213
Cornuault, N., Lehnert, M.D., Boulanger, F., Guillard, P. 2016, A&A, submitted (arXiv:1609.04405)
Corsini, E. M. 2014, Multi-Spin Galaxies, ASP Conference Series, 486, 51
Cortese, L., Fogarty, L. M. R., Ho, I.-T., et al. 2014, ApJL, 795, L37
Côté, P., Ferrarese, L., Jordán, A., et al. 2007, ApJ, 671, 1456
Ct, P., Ferrarese, L., Jordn, A., et al. 2008, in IAU Symp. 245, Formation & Evolution of Galaxy Bulges, ed. M. Bureau, E. Athanassoula & B. Barbuy (Cambridge: Cambridge Univ. Press), 395
Courteau, S., de Jong, R. S., & Broeils, A. H. 1996, ApJL, 457, L73
Croom, S. M., Lawrence, J. S., Bland-Hawthorn, J., et al. 2012, MNRAS, 421, 872
Danovich, M., Dekel, A., Hahn, O., & Teyssier, R. 2012, MNRAS, 422, 1732
Danovich, M., Dekel, A., Hahn, O., Ceverino, D., & Primack, J. 2014, MNRAS, 449, 2087
Davies, R. L., Efstathiou, G., Fall, S. M., Illingworth, G., & Schechter, P. L. 1983, ApJ, 266, 41
Davis, T. A., Alatalo, K., Sarzi, M., et al. 2011, MNRAS, 417, 882
Dekel, A., & Birnboim, Y. 2006, MNRAS, 368, 2
Dekel, A., Birnboim, Y., Engel, G., et al. 2009, Nature, 457, 451
de la Rosa, I. G., La Barbera, F., Ferreras, I., et al. 2016, MNRAS, 457, 1916
De Lucia, G., Poggianti, B. M., Halliday, C., et al. 2009, MNRAS, 400, 68
den Brok, M., Peletier, R. F., Valentijn, E. A., et al. 2011, MNRAS, 414, 3052
de Vaucouleurs, G. 1957, AJ, 62, 69
D'Onofrio, M., Marziani, P., & Buson, L. 2015, Frontiers in Astronomy and Space Sciences, 2, 4
de Rijcke, S., Michielsen, D., Dejonghe, H., Zeilinger, W. W., & Hau, G. K. T. 2005, A&A, 438, 491
De Rijcke, S., Van Hese, E., & Buyle, P. 2010, ApJL, 724, L171
Dullo, B. T., & Graham, A. W. 2014, MNRAS, 444, 2700
Djorgovski, S., & Davis, M. 1987, ApJ, 313, 59
Ebeling, H., Stephenson, L. N., & Edge, A. C. 2014, ApJL, 781, L40
Elmegreen, B.G., Struck, C. 2016, ApJ, 830, 115
Emsellem, E., Cappellari, M., Krajnović, D., et al. 2007, MNRAS, 379, 401
Emsellem, E., Cappellari, M., Krajnović, D., et al. 2011, MNRAS, 414, 888
Erwin, P., Beckman, J. E., & Pohlen, M. 2005, ApJL, 626, L81
Faber, S. M. 1973, ApJ, 179, 423
Falcón-Barroso, J., Lyubenova, M., van de Ven, G., et al. 2016, A&A, 597, A48
Fall, S. M. 1983, in IAU Symp. 100, Internal Kinematics and Dynamics of Galaxies, ed. E. Athanassoula (Cambridge: Cambridge Univ. Press), 391
Ferrarese, L., Côté, P., Jordán, A., et al. 2006, ApJS, 164, 334
Ferrarese, L. 2016, in "From the Realm of the Nebulae to Populations of Galaxies: Dialogues on a century of Research", M. D'Onofrio, R. Rampazzo, S. Zaggia (Eds.), Springer Publishing, Astrophysics and Space Science Library, v.435, p.402-407
Ferrers N.M. 1877, Quart. J. Pure Appl. Math., 14, 1
Fogarty, L. M. R., Scott, N., Owers, M. S., et al. 2015, MNRAS, 454, 2050
Forbes, D. A., Franx, M., Illingworth, G. D., & Carollo, C. M. 1996, ApJ, 467, 126
Forbes, D. A., Lasky, P., Graham, A. W., & Spitler, L. 2008, MNRAS, 389, 1924
Foster, C., Arnold, J. A., Forbes, D. A., et al. 2013, MNRAS, 435, 3587
Foster, C., Pastorello, N., Roediger, J., et al. 2016, MNRAS, 457, 147
Freeman, K.C. 1970, ApJ, 160, 811
Fukugita, M., Shimasaku, K., & Ichikawa, T. 1995, PASP, 107, 945
Fuse, C., Marcum, P., & Fanelli, M. 2012, AJ, 144, 57
Galletta, G. 1987, ApJ, 318, 531
Gavazzi, G., Boselli, A., Mayer, L., et al. 2001, ApJL, 563, L23
Gavazzi, G., Zaccardo, A., Sanvito, G., Boselli, A., & Bonfanti, C. 2004, A&A, 417, 499
Geha, M., Guhathakurta, P., & van der Marel, R. P. 2003, AJ, 126, 1794
Geha, M., van der Marel, R. P., Guhathakurta, P., et al. 2010, ApJ, 711, 361
Genel, S., Bouché, N., Naab, T., Sternberg, A., & Genzel, R. 2010, ApJ, 719, 229
Gill, S. P. D., Knebe, A., & Gibson, B. K. 2005, MNRAS, 356, 1327
González-Samaniego, A., Colín, P., Avila-Reese, V., Rodríguez-Puebla, A., & Valenzuela, O. 2014, ApJ, 785, 58
Graham, A. W. 2002, ApJL, 568, L13
Graham, A.W. 2005, in IAU Colloq. 198, Near-fields Cosmology with Dwarf Elliptical Galaxies, ed. H. Jerjen & B. Binggeli (Cambridge: Cambridge Univ. Press), 303
Graham, A.W. 2013, in "Planets, Stars and Stellar Systems", Volume 6, p.91-140, T.D.Oswalt & W.C.Keel (Eds.), Springer Publishing (arXiv:1108.0997)
Graham, A.W. 2016, in "Galactic Bulges", E. Laurikainen, R.F. Peletier & D. Gadotti (Eds.), Springer International Publishing, Astrophysics and Space Science Library, v.418, p.263-313 (arXiv:1501.02937)
Graham, A. W., Ciambur, B. C., & Savorgnan, G. A. D. 2016, ApJ, 831, 132
Graham, A. W., Colless, M. M., Busarello, G., Zaggia, S., & Longo, G. 1998, A&AS, 133, 325
Graham, A. W., Dullo, B. T., & Savorgnan, G. A. D. 2015, ApJ, 804, 32
Graham, A. W., & Guzmán, R. 2003, AJ, 125, 2936
Graham, A. W., & Guzmán, R. 2004, in Penetrating Bars Through Masks of Cosmic Dust, Edited by D.L. Block, I. Puerari, K.C. Freeman, R. Groess, and E.K. Block. Dordrecht: Kluwer Academic Publishers, ASSL, 319, 723
Graham, A. W., Jerjen, H., & Guzmán, R. 2003, AJ, 126, 1787
Graham, A. W., Merritt, D., Moore, B., Diemand, J., & Terzić, B. 2006, AJ, 132, 2711
Graham, A. W., Spitler, L. R., Forbes, D. A., et al. 2012, ApJ, 750, 121
Graham, A. W., & Worley, C. C. 2008, MNRAS, 388, 1708
Grebel, E. K., Gallagher, J. S., III, & Harbeck, D. 2003, AJ, 125, 1926
Gunn, J. E., & Gott, J. R., III 1972, ApJ, 176, 1
Held, E. V., de Zeeuw, T., Mould, J., & Picard, A. 1992, AJ, 103, 851
Hernández-Toledo, H. M., Vázquez-Mata, J. A., Martínez-Vázquez, L. A., Choi, Y.-Y., & Park, C. 2010, AJ, 139, 2525
Ho, L. C., Li, Z.-Y., Barth, A. J., Seigar, M. S., & Peng, C. Y. 2011, ApJS, 197, 21
Huchra, J. P., Macri, L. M., Masters, K. L., et al. 2012, ApJS, 199, 26
Hui, X., Ford, H. C., Freeman, K. C., & Dopita, M. A. 1995, ApJ, 449, 592
Huxor, A. P., Phillipps, S., & Price, J. 2013, MNRAS, 430, 1956
Janz, J., & Lisker, T. 2008, ApJL, 689, L25
Janz, J., & Lisker, T. 2009, ApJL, 696, L102
Janz, J., Laurikainen, E., Lisker, T., et al. 2012, ApJL, 745, L24
Janz, J., Laurikainen, E., Laine, J., Salo, H., & Lisker, T. 2016, MNRAS, 461, L82
Janz, J., Penny, S.J., Graham, A.W., Forbes, D.A., Davies, R.L. 2017, MNRAS, in press (arXiv:1703.04975)
Jarrett, T.H., Chester, T., Cutri, R., et al. 2000, AJ, 119, 2498 (2MASS)
Jarrett, T. H., Cohen, M., Masci, F., et al. 2011, ApJ, 735, 112
Jerjen, H., Kalnajs, A., & Binggeli, B. 2000, A&A, 358, 845
Jin, Y., Chen, Y., Shi, Y., et al. 2016, MNRAS, 463, 913
Karachentseva, V. E., Karachentsev, I. D., & Sharina, M. E. 2010, Astrophysics, 53, 462
Kassin, S. A., Weiner, B. J., Faber, S. M., et al. 2007, ApJL, 660, L35

Katkov, I. Y., Sil'chenko, O. K., & Afanasiev, V. L. 2014, MNRAS, 438, 2798
Katkov, I. Y., Kniazev, A. Y., & Sil'chenko, O. K. 2015, AJ, 150, 24
Kazantzidis, S., Łokas, E. L., Callegari, S., Mayer, L., & Moustakas, L. A. 2011, ApJ, 726, 98
Kazantzidis, S., Łokas, E. L., & Mayer, L. 2013, ApJL, 764, L29
Keenan, D. W., & Innanen, K. A. 1975, AJ, 80, 290
Kereš, D., Katz, N., Weinberg, D. H., & Davé, R. 2005, MNRAS, 363, 2
King, I. 1962, AJ, 67, 471
King, I. R., & Kiser, J. 1973, ApJ, 181, 27
Klimentowski, J., Łokas, E. L., Kazantzidis, S., Mayer, L., & Mamon, G. A. 2009, MNRAS, 397, 2015
Koleva, M., de Rijcke, S., Prugniel, P., Zeilinger, W. W., & Michielsen, D. 2009, MNRAS, 396, 2133
Koleva, M., Prugniel, P., de Rijcke, S., & Zeilinger, W. W. 2011, MNRAS, 417, 1643
Koleva, M., Bouchard, A., Prugniel, P., De Rijcke, S., & Vauglin, I. 2013, MNRAS, 428, 2949
Kormendy, J., & Bender, R. 2012, ApJS, 198, 2
Krajnović, D., Alatalo, K., Blitz, L., et al. 2013, MNRAS, 432, 1768
Lacerna, I., Hernández-Toledo, H. M., Avila-Reese, V., Abonza-Sane, J., & del Olmo, A. 2016, A&A, 588, A79
Lagos, C. d. P., Padilla, N. D., Davis, T. A., et al. 2015, MNRAS, 448, 1271
Lane, R. R., Salinas, R., & Richtler, T. 2015, A&A, 574, A93
Larson, R. B., Tinsley, B. M., & Caldwell, C. N. 1980, ApJ, 237, 692
Laurikainen, E., Salo, H., Buta, R., Knapen, J. H., & Comerón, S. 2010, MNRAS, 405, 1089
Laurikainen, E., Salo, H., Buta, R., & Knapen, J. H. 2011, MNRAS, 418, 1452
Liller, M. H. 1966, ApJ, 146, 28
Lisker, T., Brunngräber, R., & Grebel, E. K. 2009, Astronomische Nachrichten, 330, 966
Lisker, T., & Fuchs, B. 2009, A&A, 501, 429
Lisker, T., Grebel, E. K., & Binggeli, B. 2006, AJ, 132, 497
Łokas, E. L., Kazantzidis, S., Majewski, S. R., et al. 2010, ApJ, 725, 1516
Lu, Y., Kereš, D., Katz, N., et al. 2011, MNRAS, 416, 660
Makarova, L.N., Makarov, D.I., Karachentsev, I.D., Tully, R.B., Rizzi, L. 2016, MNRAS, 464, 2281
Maller, A. H., Katz, N., Kereš, D., Davé, R., & Weinberg, D. H. 2006, ApJ, 647, 763
Mastropietro, C., Moore, B., Mayer, L., et al. 2005, MNRAS, 364, 607
Matković, A., & Guzmán, R. 2005, MNRAS, 362, 289
Mayer, L., Governato, F., Colpi, M., et al. 2001a, ApJ, 559, 754
Mayer, L., Governato, F., Colpi, M., et al. 2001b, ApJL, 547, L123
Méndez-Abreu, J., Ruiz-Lara, T., Sánchez-Menguiano, L., et al. 2016, A&A, 598, A32
Merluzzi, P., Busarello, G., Dopita, M. A., et al. 2013, MNRAS, 429, 1747
Merluzzi, P., Busarello, G., Dopita, M. A., et al. 2016, MNRAS, 460, 3345
Merritt, D. 2006, ApJ, 648, 976
Merritt, D., & Milosavljević, M. 2005, Living Reviews in Relativity, 8, 8
Michard, R., & Marchal, J. 1993, A&AS, 98, 29
Michielsen, D., Boselli, A., Conselice, C. J., et al. 2008, MNRAS, 385, 1374
Monaco, L., Saviane, I., Perina, S., et al. 2009, A&A, 502, L9
Moore, B., Katz, N., Lake, G., Dressler, A., & Oemler, A. 1996, Nature, 379, 613
Moore, B., Lake, G., & Katz, N. 1998, ApJ, 495, 139
Moorman, C.M., Moreno, J., White, A., et al. 2016, ApJ, 831, 118
Mould, J. R., Huchra, J. P., Freedman, W. L., et al. 2000, ApJ, 529, 786
Murali, C., Katz, N., Hernquist, L., Weinberg, D. H., & Davé, R. 2002, ApJ, 571, 1
Nieto, J.-L., Capaccioli, M., & Held, E. V. 1988, A&A, 195, L1
Norris, M. A., Kannappan, S. J., Forbes, D. A., et al. 2014, MNRAS, 443, 1151
Oh, S., Yi, S.K., Cortese, L., et al. 2016, ApJ, 832, 69
Owers, M. S., Couch, W. J., Nulsen, P. E. J., & Randall, S. W. 2012, ApJL, 750, L23
Papovich, C., Labbé, I., Glazebrook, K., et al. 2016, Nature Astronomy, 1, 0003
Patterson, F.S., 1940, Harvard College Observatory Bulletin, 914, 9
Paturel, G., Petit, C., Prugniel, P., et al. 2003, A&A, 412, 45
Paudel, S., Lisker, T., Hansson, K. S. A., & Huxor, A. P. 2014, MNRAS, 443, 446
Paudel, S., Hilker, M., Ree, C. H., & Kim, M. 2016a, ApJL, 820, L19
Paudel, S., Lisker, T., Huxor, A.P., Ree, C.H. 2016b, MNRAS, 465, 1950
Paudel, S., Lisker, T., Kuntschner, H., Grebel, E. K., & Glatt, K. 2010, MNRAS, 405, 800
Paudel, S., & Ree, C. H. 2014, ApJL, 796, L14
Pedraz, S., Gorgas, J., Cardiel, N., Sánchez-Blázquez, P., & Guzmán, R. 2002, MNRAS, 332, L59
Penny, S.J., Conselice, C.J. 2008, MNRAS, 383, 247
Penny, S. J., Forbes, D. A., Pimbblet, K. A., & Floyd, D. J. E. 2014, MNRAS, 443, 3381
Penny, S.J., Masters, K.L., Weijmans, A.-M., et al. 2016, MNRAS, 462, 3955
Pichon, C., Pogosyan, D., Kimm, T., et al. 2011, MNRAS, 418, 2493
Planck Collaboration, Ade, P. A. R., Aghanim, N., et al. 2015, A&A, 594, A13
Pohlen, M., Beckman, J. E., Hüttemeister, S., et al. 2004, in Penetrating Bars Through Masks of Cosmic Dust, Edited by D.L. Block, I. Puerari, K.C. Freeman, R. Groess, and E.K. Block, Dordrecht: Kluwer Academic Publishers, Astrophysics and space science library (ASSL), 319, 713
Pota, V., Forbes, D. A., Romanowsky, A. J., et al. 2013, MNRAS, 428, 389
Prieto, J., Jimenez, R., & Haiman, Z. 2013, MNRAS, 436, 2301
Reda, F. M., Forbes, D. A., Beasley, M. A., O'Sullivan, E. J., & Goudfrooij, P. 2004, MNRAS, 354, 851
Richtler, T., Salinas, R., Lane, R. R., Hilker, M., & Schirmer, M. 2015, A&A, 574, A21
Roediger, J.C., Ferrarese, L., Côté, P., et al. 2016, ApJ, 836, 120
Romanowsky, A. J., Douglas, N. G., Arnaboldi, M., et al. 2003, Science, 301, 1696
Romanowsky, A. J., & Fall, S. M. 2012, ApJS, 203, 17
Rood, H. J. 1965, AJ, 70, 689
Ryś, A., Koleva, M., Falcón-Barroso, J., et al. 2015, MNRAS, 452, 1888
Sánchez, S. F., Kennicutt, R. C., Gil de Paz, A., et al. 2012, A&A, 538, A8
Sancisi, R., Fraternali, F., Oosterloo, T., & van der Hulst, T. 2008, A&ARv, 15, 189
Sandage, A., & Binggeli, B. 1984, AJ, 89, 919
Sanduleak, N., & Pesch, P. 1987, ApJS, 63, 809
Saviane, I., Monaco, L., & Hallas, T. 2010, in Stellar Populations – Planning for the Next Decade, G.Bruzual and S.Charlot (eds), (Cambridge: Cambridge Univ. Press), IAU Symp., 262, 426
Savorgnan, G. A. D., & Graham, A. W. 2016a, ApJS, 222, 10
Savorgnan, G. A. D., & Graham, A. W. 2016b, MNRAS, 457, 320
Schlafly, E. F., & Finkbeiner, D. P. 2011, ApJ, 737, 103
Schlegel, D. J., Finkbeiner, D. P., & Davis, M. 1998, ApJ, 500, 525
Scott, N., Davies, R. L., Houghton, R. C. W., et al. 2014, MNRAS, 441, 274
Seibert, M., Wyder, T., Neill, J., et al. 2012, American Astronomical Society Meeting Abstracts, 219, 340.01
Sellwood J.A., Wilkinson A. 1993, Rep. Prof. Phys., 56, 173
Semelin, B., & Combes, F. 2005, A&A, 441, 55
Sérsic, J. L. 1963, Boletin de la Asociacion Argentina de Astronomia La Plata Argentina, 6, 41
Sheinis, A. I., Miller, J. S., Bolte, M., & Sutin, B. M. 2000, Proc. SPIE, 4008, 522
Simien, F., & Prugniel, P. 2002, A&A, 384, 371
Simien, F., Michard, R. 1990, A&A, 227, 11
Smith, R., Davies, J. I., & Nelson, A. H. 2010, MNRAS, 405, 1723
Smith, R., Sánchez-Janssen, R., Beasley, M. A., et al. 2015, MNRAS, 454, 2502

Stewart, K. R., Brooks, A. M., Bullock, J. S., et al. 2013, ApJ, 769, 74
Stott, J. P., Smail, I., Edge, A. C., et al. 2007, ApJ, 661, 95
Teodorescu, A. M., Méndez, R. H., Saglia, R. P., et al. 2005, ApJ, 635, 290
Toloba, E., Guhathakurta, P., van de Ven, G., et al. 2014, ApJ, 783, 120
Toloba, E., Guhathakurta, P., Boselli, A., et al. 2015, ApJ, 799, 172
Toloba, E., Li, B., Guhathakurta, P. 2016, ApJ, 822, 51
van de Voort, F., Schaye, J., Booth, C. M., Haas, M. R., & Dalla Vecchia, C. 2011, MNRAS, 414, 2458
van den Bergh, S. 1976, ApJ, 206, 883
van der Kruit, P. C. 1987, A&A, 173, 59
Weiner, B. J., Willmer, C. N. A., Faber, S. M., et al. 2006, ApJ, 653, 1027
Weinmann, S. M., Lisker, T., Guo, Q., Meyer, H. T., & Janz, J. 2011, MNRAS, 416, 1197
White, S. D. M., & Frenk, C. S. 1991, ApJ, 379, 52
Wirth, A., Gallagher, J.S. 1984, ApJ, 282, 85
Woodley, K. A., Harris, W. E., Beasley, M. A., et al. 2007, AJ, 134, 494
Wright, E. L. 2006, PASP, 118, 1711
Wright, E. L., Eisenhardt, P. R. M., Mainzer, A. K., et al. 2010, AJ, 140, 1868
Yagi, M., Yoshida, M., Komiyama, Y., et al. 2010, AJ, 140, 1814
Zaritsky, D., Zabludoff, A. I., & Gonzalez, A. H. 2008, ApJ, 682, 68